REPORT DOCUMENTATION PAGE

Form Approved OMB NO. 0704-0188

1. REPORT DATE (DD-MM-YYYY)	2. REPORT TYPE	3. DATES COVERED (From - To)
02-09-2014	MS Thesis	-

4. TITLE AND SUBTITLE
On the Probability of Error and Stochastic Resonance in Discrete Memoryless Channels

5a. CONTRACT NUMBER
W911NF-11-1-0144

5b. GRANT NUMBER

5c. PROGRAM ELEMENT NUMBER
206022

6. AUTHORS
Daniel T Gebremicheal

5d. PROJECT NUMBER

5e. TASK NUMBER

5f. WORK UNIT NUMBER

7. PERFORMING ORGANIZATION NAMES AND ADDRESSES
The University of the District of Columbia
Computer Science and Informati
Briana Lowe Wellman
Washington, DC 20008 -1122

8. PERFORMING ORGANIZATION REPORT NUMBER

9. SPONSORING/MONITORING AGENCY NAME(S) AND ADDRESS (ES)
U.S. Army Research Office
P.O. Box 12211
Research Triangle Park, NC 27709-2211

10. SPONSOR/MONITOR'S ACRONYM(S)
ARO

11. SPONSOR/MONITOR'S REPORT NUMBER(S)
58962-NS-REP.12

12. DISTRIBUTION AVAILIBILITY STATEMENT
Approved for public release; distribution is unlimited.

13. SUPPLEMENTARY NOTES
The views, opinions and/or findings contained in this report are those of the author(s) and should not contrued as an official Department of the Army position, policy or decision, unless so designated by other documentation.

14. ABSTRACT
In this thesis, we studied the performance of Discrete Memoryless Channels (DMC), arising in the context of cooperative underwater wireless sensor networks. We formulated an analytic relationship that relates the average probability of error to the systems parameters, the signal amplitude, the decision threshold and the noise power values. First we studied the trade-off between the signal amplitude and the decision threshold in the special case (2, 2) DMC. Following our (2, 2) DMC model we proposed a symmetric decision threshold to formulate our analytical relationship for the average probability of error based on four arbitrarily defined regions of interest. In order to

15. SUBJECT TERMS
Discreeete Memoryles Channels, Underwater Communication

16. SECURITY CLASSIFICATION OF:			17. LIMITATION OF ABSTRACT	15. NUMBER OF PAGES	19a. NAME OF RESPONSIBLE PERSON
a. REPORT	b. ABSTRACT	c. THIS PAGE			Paul Cotae
UU	UU	UU	UU		19b. TELEPHONE NUMBER 202-274-6290

Standard Form 298 (Rev 8/98)
Prescribed by ANSI Std. Z39.18

Report Title

On the Probability of Error and Stochastic Resonance in Discrete Memoryless Channels

ABSTRACT

In this thesis, we studied the performance of Discrete Memoryless Channels (DMC), arising in the context of cooperative underwater wireless sensor networks. We formulated an analytic relationship that relates the average probability of error to the systems parameters, the signal amplitude, the decision threshold and the noise power values. First we studied the trade-off between the signal amplitude and the decision threshold in the special case (2, 2) DMC. Following our (2, 2) DMC model we proposed a symmetric decision threshold to formulate our analytical relationship for the average probability of error based on four arbitrarily defined regions of interest. In order to design a resilient system, conditional probabilities of error are defined with respect to the optimum zero threshold in the (2, 3) DMC.

We analyzed the stochastic resonance (SR) phenomenon impact upon the performance limits of a distributed underwater wireless sensor networks operating with limited transmitted power and computational capabilities. We focused on the threshold communication systems where, due to the underwater environment, non-coherent communication techniques are affected both by noise and threshold level. The binary-input ternary-output channel is used as a theoretical model for the DMC.

To further deduce the relationship between the signal amplitude and the decision threshold, we classified the average probability of error into its respective probabilities of interest; the probability of false alarm, probability of correct detection, probability of miss and probability of correct rejection. We studied how the probability of correct detection and false alarm varies with our symmetric decision threshold theta and the noise variance sigma. In addition to that we investigated how the probability of correct rejection and miss varies with our system parameters.

We also investigated how a sub threshold/super threshold signal determines the optimum system performance in the case of the (2, 2) and the (2, 3) DMCs. We found the optimum value of the additive noise power that results in a better system performance in bistable systems as function of detector threshold and the signal amplitude.

Our findings show how the combination of the (2, 2) DMC and the simple symmetric (2, 3) DMC yields a better signal detection in the presence of additive Gaussian noise. In the case of our proposed (2, 3) DMC for the underwater distributed wireless sensor networks, the probability associated with zero optimum crossing threshold remains constant. Thus, in order for the probability of detection to be maximized by minimizing the probability of false alarm and miss, the detection scheme needs to incorporate suprathreshold signal and symmetric threshold around the zero optimum threshold in the case of (2, 2) DMC.

On the Probability of Error and Stochastic Resonance in Discrete Memoryless Channels

By

Daniel T Gebremicheal

A thesis submitted To Graduate Faculty of the

University of the District of Columbia

in Partial Fulfillment of the

Requirements for the Degree of

Master of Science in

Electrical Engineering

Washington, DC

December, 2013

On the Probability of Error and Stochastic Resonance in Discrete Memoryless Channels

Daniel T Gebremicheal

In this thesis, we studied the performance of Discrete Memoryless Channels (DMC), arising in the context of cooperative underwater wireless sensor networks. We formulated an analytic relationship that relates the average probability of error to the systems parameters, the signal amplitude, the decision threshold and the noise power values. First we studied the trade-off between the signal amplitude and the decision threshold in the special case (2, 2) DMC. Following our (2, 2) DMC model we proposed a symmetric decision threshold to formulate our analytical relationship for the average probability of error based on four arbitrarily defined regions of interest. In order to design a resilient system, conditional probabilities of error are defined with respect to the optimum zero threshold in the (2, 3) DMC.

We analyzed the stochastic resonance (SR) phenomenon impact upon the performance limits of a distributed underwater wireless sensor networks operating with limited transmitted power and computational capabilities. We focused on the threshold communication systems where, due to the underwater environment, non-coherent communication techniques are affected both by noise and threshold level. The binary-input ternary-output channel is used as a theoretical model for the DMC.

To further deduce the relationship between the signal amplitude and the decision threshold, we classified the average probability of error into its respective probabilities of interest; the probability of false alarm, probability of correct detection, probability of miss and probability of correct rejection. We studied how the probability of correct detection and false alarm varies with our symmetric decision threshold theta and the noise variance sigma. In addition to that we investigated how the probability of correct rejection and miss varies with our system parameters.

We also investigated how a sub threshold/super threshold signal determines the optimum system performance in the case of the (2, 2) and the (2, 3) DMCs. We found the optimum value of the additive noise power that results in a better system performance in bistable systems as function of detector threshold and the signal amplitude.

Our findings show how the combination of the (2, 2) DMC and the simple symmetric (2, 3) DMC yields a better signal detection in the presence of additive Gaussian noise. In the case of our proposed (2, 3) DMC for the underwater distributed wireless sensor networks, the probability associated with zero optimum crossing threshold remains constant. Thus, in order for the probability of detection to be maximized by minimizing the probability of false alarm and miss, the detection scheme needs to incorporate suprathreshold signal and symmetric threshold around the zero optimum threshold in the case of (2, 2) DMC.

Acknowledgments

I would like to express my deepest gratitude to my advisor, Dr.Paul Cotae, for his excellent guidance, caring and patience. Also I am thankful to the Department of Defense (DoD) Grant W911NE-11-1-0144 for their financial support throughout my master's program.

My sincere thanks go of the Naval Research Laboratory, Dr. Ira S. Moskowitz.

I would like to acknowledge the Electrical and Computer Engineering Department which has been helpful throughout my master degree, especially Dr. Samuel Lakeou, Dr. Sasan Haghani and Dr. Esther Ososanya.

I would also like to thank my parents and my siblings. They were always helpful and encouraging me with their best wishes.

Contents

List of Figures

List of Abbreviations and Notations

AGN	Additive Gaussian Noise
BAC	Binary Asymmetric Channel
BER	Bit Error Rate
BSC	Binary Symmetric Channel
BW	Bandwidth of a Channel
C(X, Y)	Capacity of a channel with input X and output Y
dB	Decibel
FIT	Forbidden Interval Theorem
I_r	Intensity of Sound at the receiver
I_t	Intensity of Sound at the transmitter
(M, N)	DMC Discrete Memoryless Channel with m inputs and n outputs
N_0	Power spectral density of noise
P	Power of a signal
PDF	Probability density function
P_{fa}	Probability of false alarm
P_d	Probability of detection
P_{dt}	Probability of true detection
P_e	Average probability of error
P_m	Probability of miss
P_r	Probability of rejection
ROC	Receiver operating characteristics curve
SR	Stochastic resonance
TL	Transmission loss

Summary

In this thesis, we studied the performance of Discrete Memoryless Channels (DMCs), arising in the context of cooperative underwater wireless sensor networks. We formulated an analytic relationship that relates the average probability of error to the systems parameters, the signal amplitude, the decision threshold and the noise power values. We first studied the trade-off between the signal amplitude and the decision threshold in the special case (2, 2) DMC. Following our (2, 2) DMC model we proposed a symmetric decision threshold in order to find the average probability of error based on four arbitrarily defined regions of interest. In order to design a resilient system condition probabilities of error are defined with respect to the optimum zero threshold in the (2, 3) DMC.

We analyzed the stochastic resonance (SR) phenomenon impact upon the performance limits of a distributed underwater wireless sensor networks operating with limited transmitted power and computational capabilities. We focused on the threshold communication systems where, due to the underwater environment, non-coherent communication techniques are affected both by noise and threshold level. The binary-input ternary-output channel is used as a theoretical model for the DMC.

To further deduce the relationship between the signal amplitude and the decision threshold, we classified the average probability of error into its respective probabilities of interest; the probability of false alarm, probability of correct detection, probability of miss and probability of correct rejection. We studied how the probability of correct detection and false alarm varies with our symmetric decision threshold theta and the noise variance sigma. In addition to that we investigated how the probability of correct rejection and miss varies with our system parameters.

We also investigated how a sub threshold/super threshold signal determines the optimum system performance in the case of the (2, 2) and the (2, 3) DMCs. We found the optimum value of the additive noise power that results in a better system performance in bistable systems as function of detector threshold and the signal amplitude.

Our findings show how the combination of the (2, 2) DMC and the simple symmetric (2, 3) DMC yields a better signal detection in the presence of additive Gaussian noise. In the case of our proposed (2, 3) DMC for the underwater distributed wireless sensor networks, the probability associated with zero optimum crossing threshold remains constant. Thus, in order for the probability of detection to be maximized by minimizing the probability of false alarm and miss, the detection scheme needs to incorporate suprathreshold signal and symmetric threshold around the zero optimum threshold in the case of (2, 2) DMC.

Chapter 1

Introduction

In this thesis, we investigated probability of error and Stochastic Resonance (SR) effect for the binary-input ternary-output (2, 3) Discrete Memoryless Channel (DMC). We revisited the BSC which is a special case of the (2, 3) DMC. We studied how the probability of error varies for fixed value of the threshold as the signal to noise ratio increases. We investigated the trade-off between the signal amplitude and the decision threshold value for a different value of noise power.

In order to study SR, we modeled the (2, 3) DMC by a physical communication channel. We proposed a symmetric decision threshold and conditional probabilities in order to maximize target detection and tracking in the case of underwater distributed wireless sensor networks. In the presence of a Gaussian noise, the SR phenomenon is observed over a certain range of threshold values. We focused on the additive Gaussian noise in which case we determined the interval under which our system exhibit SR. The main contributions of this thesis consist in deriving the average probability of error in the (2, 3) DMC and determining the interval by which the SR effect is observed.

1.1 Thesis Structure

The rest of the thesis is structured as follows

Chapter 2 provides the background concepts and the literature reviews, which will be used throughout the thesis. We also review the (2, 2) DMC.

Chapter 3 reviews and derives the probability of error in the (2, 3) DMC. We investigate the tradeoff between the signal amplitude and the decision threshold for optimum system performance. We deduce the relationship between the signal amplitude and the decision threshold theta. Moreover, we investigate how the probabilities of false alarm and detection vary with respect to the symmetric decision threshold theta. Similarly we study how the probability of miss and correct rejection are also affected by the selection of the threshold Θ and noise power σ.

Chapter 4 analyzes the effects of SR and the physical model of the (2, 3) DMC in presence of Gaussian noise. We compare the performance of the (2, 2) and (2, 3) DMCs in the context of SR. Also we derive the optimum value of the noise that results in SR in the case of the (2, 2) DMC and the (2, 3) DMC. We also check the fundamental theorem in the case of SR, the forbidden interval theorem (FIT).

Chapter 5 engages a discussion about the results and future work which can enhance the signal detection and application of our proposed (2, 3) DMC in the case of underwater distributed wireless sensor networks.

1.2 Thesis Significance and Contribution

This research contributes to Dr. Cotae's research titled "Information - Driven Doppler Shift Estimation and Compensation Methods for Underwater Wireless Sensor Networks", which is to analyze and develop noncoherent communication methods at the physical layer for target tracking and use the information theory tools to predict the next target position by processing the data information collected from a collaborative wireless distributed sensor network [4]. It improves the understanding of the physical communication model in the case of (2, 3) DMCs. In addition, it contributes to the improvement of the performance limits of distributed underwater wireless sensor networks, by maximizing the probability of target detection and tracking in the presence of additive Gaussian noise. Moreover, we compare the performance of the different DMCs for better signal detection in underwater wireless sensors, operating with limited transmitted power and computational environment. The results of this work will contribute to the effort of overcoming the effect of noise in underwater sensors and signal processing.

In Chapter 3 we derive (33), the analytic relationship for the probability of error in the (2, 3) DMC. We investigate how the selection of the threshold with respect to the signal amplitude affects the average probability of error. We show how our new model improves signal detection by defining symmetric conditional probabilities around the zero optimum threshold in the case of the (2, 3) DMC.

Our findings show how the combination of the (2, 2) DMC and the simple symmetric (2, 3) DMC yields a better signal detection in the presence of additive Gaussian noise. In the case of our proposed (2, 3) DMC for the underwater distributed wireless sensor networks, the probability associated with zero optimum crossing threshold remains constant. Thus in order for probability of detection to be maximized by minimizing the probability of false alarm and miss, the detection scheme needs to incorporate suprathreshold signal and a symmetric decision threshold around the zero optimum threshold in the case of (2, 2) DMC.

Chapter 2

Background

In this chapter, we give back ground review on concepts used throughout the thesis. Under Water Channel, Probability of Error, Threshold devices, Discrete Memoryless Channels are reviewed. In addition we discuss Stochastic Resonance effect in nonlinear systems.

2.1 General Communication Systems Model

Electrical communication systems are designed to send messages or information from a source that generates the messages to one or more destinations. The information generated by the source may be of the form of voice (speech source), a picture (image source). An essential feature of any source that generates information is that its output is described in probabilistic terms; i.e., the output of a source is not deterministic. Otherwise, there would be no need to transmit the message. The structure of the communication system as shown in Figure 1 consists of three basic parts, namely, the transmitter, the channel and the receiver. The functions performed by these three elements are described below.

Transmitter: The transmitter converts the electrical signal into a form that is suitable for transmission through the physical channel or transmission medium.

Receiver: The function of the receiver is to recover the message signal contained in the transmitted signal. If the message signal is transmitted by carrier modulation, the receiver performs carrier demodulation in order to extract the message from the sinusoidal carrier.

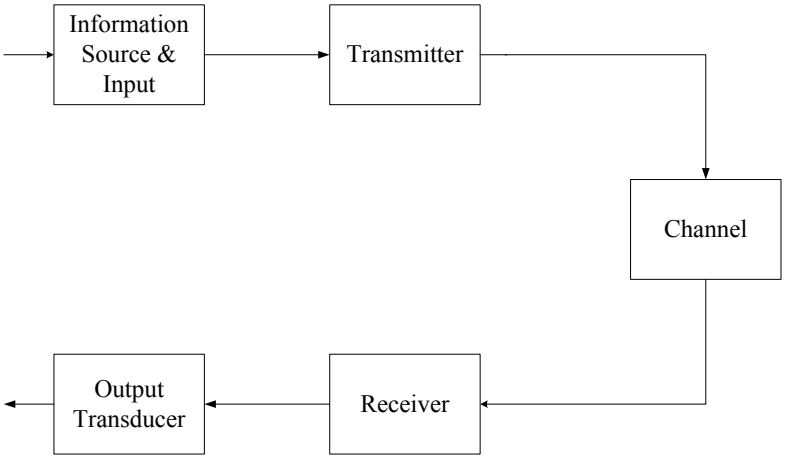

Figure 1: General communication systems model.

2.2 Communication Channel

A communication channel refers either to a physical transmission medium such as a wire, or to a logical connection over a multiplexed medium such as a radio channel as shown in the figure above. A channel is used to convey an information signal, for example a digital bit stream, from one or several senders (or transmitters) to one or several receivers. A channel has a certain capacity for transmitting information, often measured by its bandwidth in Hz or its data rate in bits per second. Depending on the type of the message transmitted, a communication channel is classified as a continuous, discrete and mixed channel.

2.3 The types of Signal Propagation in Underwater

There are three types of transmission medium in underwater communication which are acoustic communication (sound), radio wave communication (electromagnetic) and optical communication (light). Radio wave and optical communication does not work well in deep underwater environment. Thus, acoustic communication is widely chosen in deep underwater environment due to the low attenuation of sound in water.

Although radio wave communication has faster propagation speeds compared to the acoustic communication, there are limitation factors when using electromagnetic wave in deep underwater. Electromagnetic waves strongly attenuate, especially in salt water and propagating long distances require large antenna and high transmitter power.

Optical communications has a greater advantage in data rate that can exceed 1 Giga Hz. However, when used in underwater environment, the light is rapidly absorbed and the communication is affected by its scattering.

2.4 Underwater Acoustic Channels

In recent years, there has been an immense interest in developing underwater acoustic communication systems, most of which are related to remote control and telemetry applications [2].Other applications include ocean-bottom survey and marine monitoring, collection of scientific data acquired by underwater sensors without the need for retrieving the equipment. However, for all these applications the main objective is to achieve reliable communication both in point-to-point links, and in network scenarios. In practice, the only feasible method to achieve underwater communications is by means of acoustic signals. Such acoustic links are exposed to adverse physical phenomena governing acoustic wave propagation in the sea. These include ambient noise, frequency-dependent attenuation, temperature and pressure variations, reverberation, and extended multi-path. Any successful acoustic sensor network design must

consider all these effects in order to select an appropriate configuration for system-related parameters. The transmit power level and operating frequency must be considered in conjunction with the ambient noise and transmission range, the utilized modulation scheme, data rate, and the level of diversity must properly match the expected channel conditions related to time and frequency dispersion.

The underwater acoustic communication channel is extremely complex in nature. The complexity arises from the fact that the channel is not perfectly homogeneous. The numerous imperfections are mainly due to density and temperature gradients and the non-homogeneities of the water due to suspended particles of solid or gaseous matter. The constant water motion and the channel boundaries such as the bottom and the surface further increase the complexity. Data in UWC suffers from multipath, noise, fading, Doppler spread, and high and variable propagation delay. The factors affecting UWC establish temporal and spatial variability of the acoustic channel. The temporal and spatial variability makes the channel very limited and highly dependent on both transmission range and frequency. When viewed from a communication system designer's point of view, the four aspects that are of fundamental concern are namely, ambient noise, multi-path phenomenon, transmission loss and Doppler spreading due to relative motion between transmitter and receiver.

2.4.1 Ambient Noise

Ambient noise influences the received signal to noise ratio and largely controls the transmitter power. It generally decreases in frequency over the range of interest. Inshore environment and marine worksites are noisier than deep ocean environment and the communication system design needs to cater for the worst case.

For band limited additive white Gaussian noise (AWGN), mathematically channel capacity is expresses as

$$C = BW log_2 \left(1 + \frac{P}{N_0 BW}\right) \text{ bits/sec} \quad (1)$$

where 'C' is channel capacity, 'BW' is bandwidth, 'P' is the power of signal and 'N_0' is the power of noise. Traditionally engineers have been interested to eliminate the effect of noise in order to improve system performance. In our work we investigated the effect of noise in order to maximize the detection of the received signal by employing binary input ternary output discrete memoryless channels.

2.4.2 Multi-path phenomenon causing Inter-Symbol Interference and Reverberation

This is the most challenging aspect of the underwater acoustic channel. The boundaries of the surface and bottom reflect the energy; so numerous travel paths exist between the transmitter and the receiver. This is further complicated by imperfect boundaries. The whole phenomenon results in time dispersal of the signal. This time spreading can be as high as hundreds of milliseconds in shallow water to several seconds in deep waters. At high frequency, the total time spread is less due to absorption at boundaries and attenuation in water.

2.4.3 Transmission Loss due to geometrical spreading and absorption

The acoustic wave reduces in intensity as it propagates through the medium due to geometrical spreading and absorption mechanism. Though the attenuation of acoustic waves in water is negligible as compared to the radio wave in water, there is considerable loss in energy due to absorption mechanism in water. The loss due to geometrical spreading can be either spherical or cylindrical in nature.

Transmission loss (TL) for acoustic communication is generally expressed as the logarithmic ratio of the intensity of sound at the reference range one meter away from the center of the source (I_t) to the intensity of the sound at the receiver (I_r). TL is measured in decibels (dB). Mathematically it can be expressed as follows:

$$TL = 10 \log \left(\frac{I_t}{I_r} \right) \ dB \tag{2}$$

2.4.4 Doppler spreading due to relative motion between transmitter and receiver

This is introduced by relative motion between the transmitter and receiver, or by motion of the water. Due to the scarcity of channel bandwidth (caused by absorption losses and projector transducer characteristics), Doppler spread may easily result in further reduction in available bandwidth.

Due to harsh underwater acoustic medium described above, many well-known communication techniques cannot be applied and hence the design is a compromise between data rate, reliability and distance. The combined effects of the above mentioned phenomenon have led in the past to system design based exclusively on noncoherent detection and low signaling rates.

Approaches to system design depend upon the technique used for overcoming the effects of multi-path and time variations:

- the signal design, i.e., the choice of modulation / detection method
- the transmitter / receiver structure

2.5 Discrete Data Transmission

Discrete data transmission as shown in figure below is the transmission of one message from a finite set of messages through a communication channel. A message sender at the transmitter communicates with a message receiver. The sender selects one message from the finite set, and the transmitter sends a corresponding signal (or waveform) that represents this message through the communication channel. The receiver decides the message sent by observing the channel output. Successive transmission of discrete data messages is known as digital communication. Based on the noisy received signal at the channel output, the receiver uses a procedure known as detection to decide which message, or sequence of messages, was sent. Optimum detection minimizes the probability of an erroneous receiver decision on which message was transmitted.

The channel distorts the transmitted signals both deterministically and with random noise. The noisy channel output will usually not equal the channel input and will be described only in terms of conditional probabilities of various channel-output signals. The channel-input signals have probabilities equal to the probabilities of the messages that they represent. The optimum detector will depend only on the probabilistic model for the channel and the probability distribution of the messages at the channel input. The general optimum detector specializes in many important practical cases of interest.

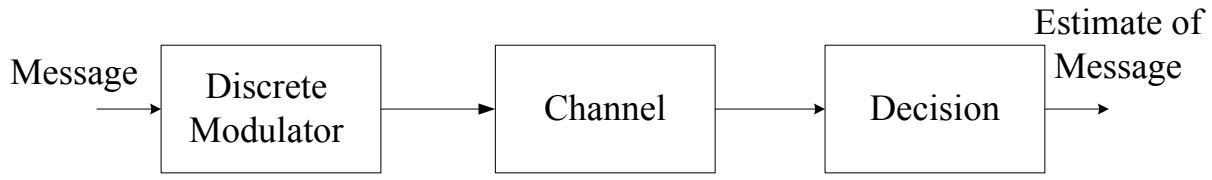

Figure 2: Block diagram of discrete data transmission.

2.5.1 Discrete Memoryless Channels

The fundamental model describing communication over a noisy channel is the so-called discrete memoryless channel (DMC). A DMC consists of :

- a finite input alphabet described by the random variable x
- a finite output alphabet described by the random variable y
- a conditional probability distribution $P(y|x)$

For a memoryless channel, the output y_i depends on the input x_i at the same time i. Therefore, the conditional probability distribution is given by

$$P(y|x) = \prod_i^n P(y_i|x_i) \tag{3}$$

where n is the number of symbols in the alphabet,

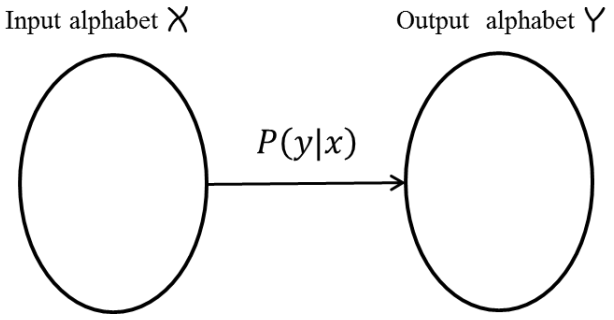

Figure 3: Discrete memoryless channel.

2.5.2 DMC General Model (M, N)

The input of a DMC is random variable x, who selects its value from a limited discrete set X, as shown in the Figure 4. All the transition probabilities from x_i to y_j are gathered in a transition matrix $p(y|x)$.The (i, j) entry of the matrix is $P(= y_j|X = x_i)$ which is called forward transition probability.

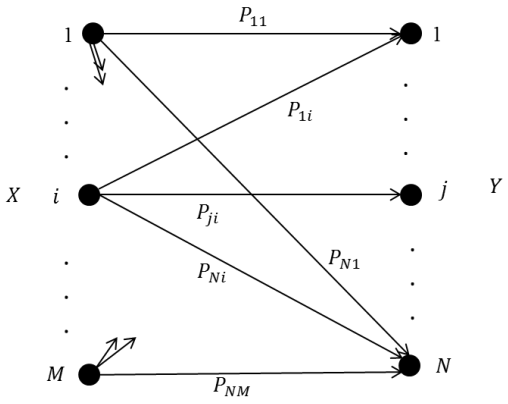

Figure 4: DMC general model.

The general DMC is called memoryless because the current output y_j depends only on the current input i.

The capacity of DMC, $p(y|x)$ is defined by

$$C = max_{p(x)} I(X;Y) \tag{4}$$

where $I(X;Y)$ is the mutual information of the two discrete random variables X and Y given by [19]

$$I(X;Y) = \sum_{y\varepsilon Y} \sum_{x\varepsilon X} P(x,y) \log\left(\frac{P(x,y)}{P(x)P(y)}\right) \tag{4.1}$$

and the maximum is taken over all input distribution-$P(x)$.

2.5.3 DMC I

Let $\mathcal{X}$ and $\mathcal{Y}$ be discrete alphabets and $P(y|x)$ be a transition probability from $\mathcal{X}$ to $\mathcal{Y}$. A discrete channel $P(y|x)$ is single-input single-output with input random variable X taking values in $\mathcal{X}$ and output random variable Y as shown in Figure 5 taking values in $\mathcal{Y}$ such that

$$P_r\{X = x, Y = y\} = P_r\{X = x\}P(y|x) \tag{5.1}$$

where $P_r(.)$ is the probability of a random variable.

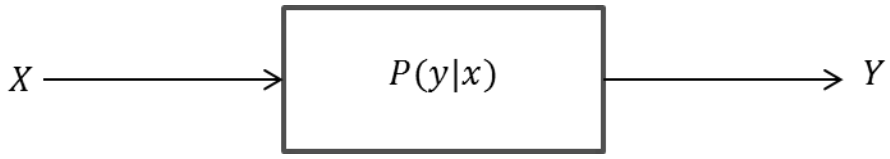

Figure 5: DMC I.

2.5.4 DMC II

Let $\mathcal{X}$, $\mathcal{Y}$, and $\mathcal{Z}$ be discrete alphabets, and $P(y|x)$ be a transition matrix. Let α: $\mathcal{X} \times \mathcal{Z} \rightarrow \mathcal{Y}$ and Z be a random variable taking values in $\mathcal{Z}$. A discrete channel (α, Z) is a single-input

single-output system with input X and output Y as shown in Figure 6. For any input random variable x, the noise variable z is independent of x, and the output random variable Y is given by

$$Y = \alpha(X, Z) \tag{5.2}$$

Where (α, Z) is a sequence of replicates of generic discrete channel (α, Z)

X_i and Y_i respectively represent the input and output of the DMC at time i.

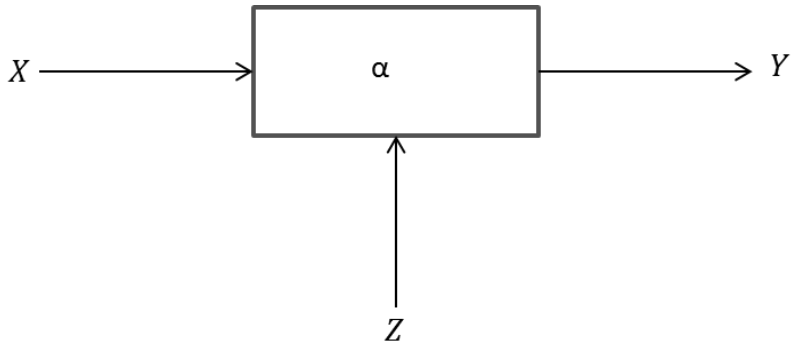

Figure 6: DMC II.

2.5.5 Example of DMC; binary –input binary-output (2, 2) DMC

A binary symmetric channel (or BSC) as shown in Figure 7 is a common communications channel model used in coding theory and information theory. In this model, a transmitter wishes to send a bit (a zero or a one), and the receiver receives a bit. It is assumed that the bit is usually transmitted correctly, but that it will be "flipped" with a small probability (the "crossover probability")$p < \frac{1}{2}$. This channel is used frequently in information theory because it is one of the simplest channels to analyze.

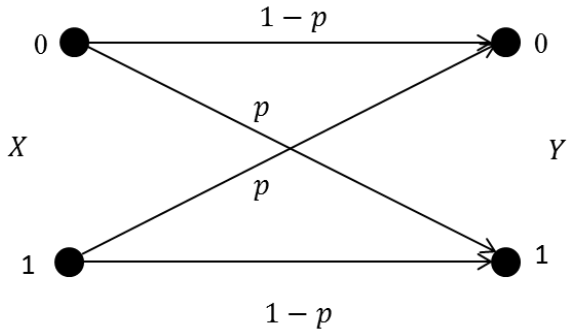

Figure 7: (2, 2) Binary symmetric channel.

There is no feedback link from the receiver back to the transmitter that would inform the transmitter about the last outputs. The transition probabilities from X to Y are given below

$$1 - p = P_r(Y = 0|X = 0) = P_r(Y = 1|X = 1) \quad (6.1)$$

where $P_r(Y = y|X = x)$ represents the probability of receiving y given the signal x was transmitted. Similarly

$$p = P_r(Y = 0|X = 1) = P_r(Y = 1|X = 0) \quad (6.2)$$

The channel transition matrix, M of the BSC is given by

$$M = \begin{pmatrix} 1-p & p \\ p & 1-p \end{pmatrix} \quad (6.4)$$

The capacity 'C' of the channel can be calculated to be [19]

$$C = 1 + p \times \log_2 p + (1-p) \times \log_2(1-p) \text{ Bits/transmission.} \quad (6.4)$$

The binary symmetric channel is one of the simplest noisy channels to analyze. Many problems in communication theory can be reduced to a BSC. Conversely, being able to transmit effectively over the BSC can give rise to solutions for more complicated channels.

2.5.6 Additive White Gaussian Noise Channel (AWGN)

Perhaps the most important, and certainly the most analyzed, digital communication channel is the AWGN channel shown in Figure 8. This channel passes the sum of the modulated signal $X(t)$ and additive Gaussian noise $N(t)$ to the output. The Gaussian noise is assumed to be uncorrelated with itself (or "white") for any non-zero time offset.

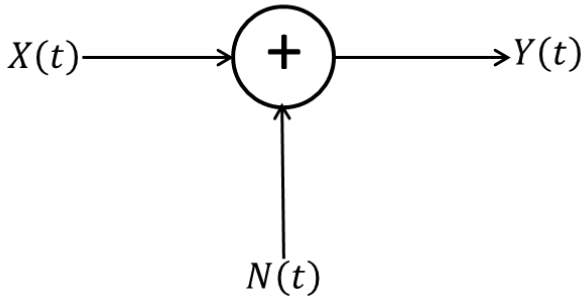

Figure 8: AWGN Channel.

This is a time discrete-channel with output Y_i at time i, where Y_i is the sum of the input X_i and the noise N_i. The noise N_i is drawn i.i.d. with a Gaussian distribution with variance σ^2 .

$$Y_i = X_i + N_i \qquad \text{where } N_i \sim (0, \sigma^2) \tag{6.5}$$

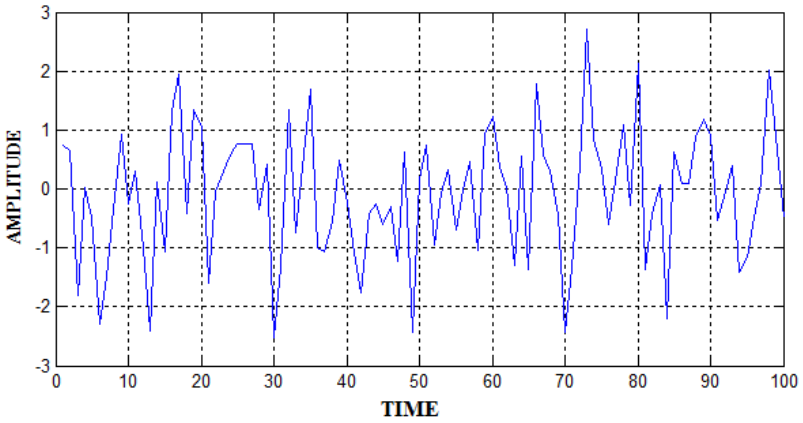

Figure 9: AWGN, $N \sim (0, 1)$.

Figure 9 shows a Gaussian noise with zero mean and variance 1.

2.6 Bit Error Rate (BER)

In digital transmission, the number of bit errors is the number of received bits of a data stream over a communication channel that has been altered due to noise, interference, distortion or bit synchronization errors. In our study of Discrete Memoryless Channels (DMC) in Chapter 3 we used the average bit error rate as performance measure to investigate the (2,3) DMC in the presence of Additive Gaussian noise.

2.6.1 Factors affecting bit error rate

In a communication system, the receiver side BER may be affected by:

- transmission channel noise,
- interference, distortion,
- bit synchronization problems,
- Attenuation, wireless multipath fading, etc.

The BER may be improved by choosing a strong signal strength (unless this causes cross-talk and more bit errors), by choosing a slow and robust modulation scheme or line coding scheme, and by applying channel coding schemes such as redundant forward error correction codes.

The transmission BER is the number of detected bits that are incorrect before error correction, divided by the total number of transferred bits (including redundant error codes).The information BER, approximately equal to the decoding error probability, is the number of decoded bits that remain incorrect after the error correction, divided by the total number of decoded bits (the useful information). Normally the transmission BER is larger than the information BER.

2.6.2 Hypothesis testing

In statistics, a type I error (or error of the first kind) is the incorrect rejection of a true null hypothesis. A type II error (or error of the second kind) is the failure to reject a false null hypothesis. A type I error is a false positive. Usually a type I error leads one to conclude that a supposed effect or relationship exists when in fact it doesn't**.** In digital communication systems type I and type II errors are analogous to probabilities of false alarm and miss respectively.

In underwater distributed wireless sensor networks where target detection and tracking is so important [4], the probability of false alarm and detection plays an important role. The first hypothesis is denoted as the null hypothesis H_0 and the second as H_1. The detection logic therefore must examine each sensor measurement to be tested and select one of the hypotheses as "best" accounting for that measurement. If H_0 best accounts for the data, the system declares that a target was not present at the range, angle, or Doppler coordinates of that measurement; if H_1 best accounts for the data, the system declares that a target was present.

The analysis starts with a statistical description of the probability density function (pdf) that describes the measurement to be tested under each of the two hypotheses. If the sample to be tested is denoted as y, then $f(y|S_1)$ and $f(y|S_1)$ are required to model the detection scheme as shown in Figure 10. The binary digits 0 and 1 are represented by voltage waveforms S_0 and S_1 respectively.

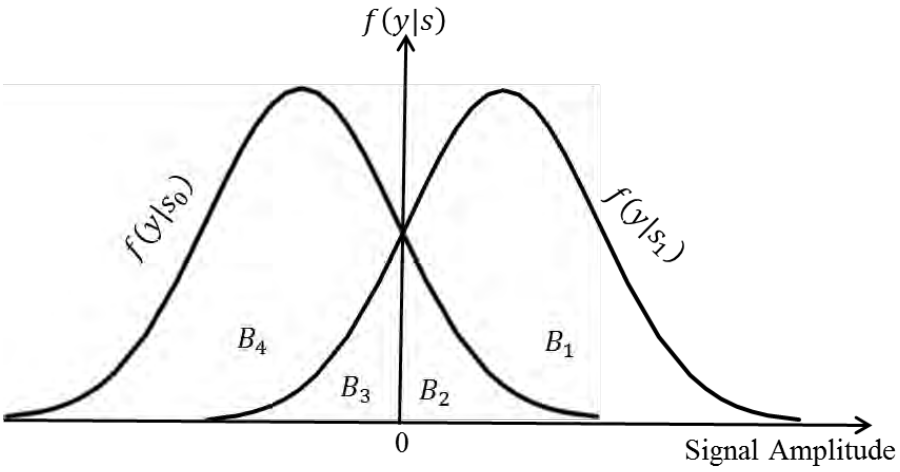

Figure 10: Zero crossing detection scheme.

As shown in figure above the detection problem is to develop models for these two pdfs. In fact, analysis of underwater distributed wireless sensor networks performance is dependent on estimating these pdfs for the system and scenario at hand. Furthermore, a good deal of the (2, 3) DMC system design problem is aimed at manipulating these two pdfs in the presence of additive white Gaussian noise in order to obtain the most favorable detection performance by minimizing probability of error.

2.7 Different probabilities of error

Once the two pdfs are successfully modeled, the following probabilities of interest can be defined: probabilities of detection, false alarm, miss and rejection.

2.7.1 Probability of true detection (P_{dt})

The probability that a target is declared (i.e., S_1 is chosen) when a target is in fact present. This is the area $(B_1 + B_2)$ by which the pdf, $f(y|S_1)$ is greater than the decision threshold Θ as shown in Figure 10.

$$P_{dt} = \int_0^{\infty} f(y|S_1)dy \tag{7}$$

where $f(y)$ is the probability density function of the normally distributed Gaussian random variable with mean μ and variance σ^2

$$f(y|S) = \frac{1}{\sqrt{2\pi\sigma^2}} \times e^{\frac{-(y-A)^2}{2\sigma^2}} \tag{8}$$

Thus the probability of detection can be reduced into

$$P_{dt} = \int_0^{\infty} \frac{1}{\sqrt{2\pi\sigma^2}} \times e^{\frac{-(y-A_1)^2}{2\sigma^2}} dy \quad (9)$$

2.7.2 Probability of false alarm (P_{fa})

The probability that a target is declared (i.e., S_1 is chosen) when a target is in fact not present. It is the area (B_2) by which the Pdf, $f(y|S_0)$ is greater than the decision threshold Θ as shown in Figure 10.

$$P_{fa} = \int_0^{\infty} f(y|S_0)dy \quad (10)$$

Using (8) the probability of false alarm is mathematically defined as

$$P_{fa} = \int_0^{\infty} \frac{1}{\sqrt{2\pi\sigma^2}} \times e^{\frac{-(y-A_0)^2}{2\sigma^2}} dy \quad (11)$$

2.7.3 Probability of miss (P_m)

The probability that a target is not declared (i.e., S_0 is chosen) when a target is in fact present. This is the area (B_2) by which the Pdf,$f(y|S_1)$ is less than the decision threshold Θ as shown in Figure 10.

2.7.4 Probability of rejection (P_r)

The probability that a target is not declared (i.e., S_0 is chosen) when a target is not present. This is the area ($B_3 + B_4$) by which the Pdf,$f(y|S_0)$ is less than the decision threshold theta as shown in figure above.

Note that $P_m = 1 - P_{dt}$ and $P_r = 1\text{-}P_{fa}$. Thus, P_{dt} and P_{fa} are suffice to specify all of the probabilities of interest. As the latter two definitions imply, it is important to realize that, because the problem is statistical, there will be a finite probability that the decisions will be wrong. Thus by adjusting our threshold Θ and the noise power σ, the (2, 3) DMC can achieve a better performance in minimizing the average probability of error.

2.8 Binary-input binary output DMC and average probability of error

The (2, 2) DMC is shown in Figure 11. It is characterized by the input random variable X and the output random variable Y, taking values (x_1, x_2) and (y_1, y_2), respectively. Its transition probability matrix M is defined by

$$M(\alpha,\beta) = \begin{bmatrix} \alpha & 1-\alpha \\ \beta & 1-\beta \end{bmatrix} = \begin{bmatrix} \alpha & \bar{\alpha} \\ \beta & \bar{\beta} \end{bmatrix} \tag{12.1}$$

where α and β are defined as:

$$\alpha = P(Y = y_1 | X = x_1),\ \beta = P(Y = y_2 | X = x_2) \tag{12.2}$$

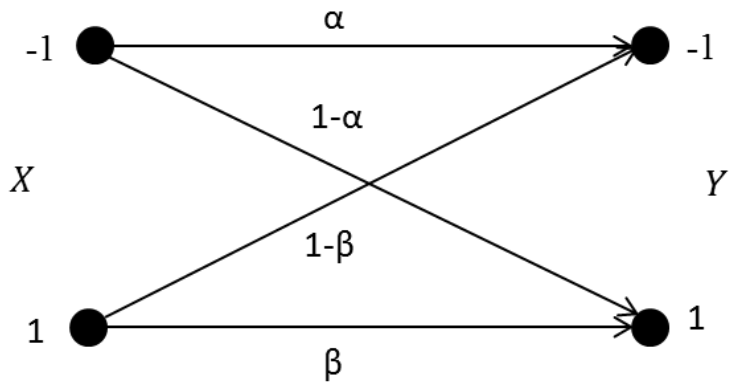

Figure 11: Binary asymmetric channel.

For the Binary input-binary output asymmetric channel, a simple threshold based detection detector can be employed as shown in the Figure 12 to study its performance and investigate the effect of noise, which could be a corner stone in the discussion of the (2, 3) DMC that will follow.

In the (2, 2) DMC the source maps the bits 0 and 1 into voltage levels –A and A respectively as shown in Figure 11.The massage is transmitted across the channel where there is an additive white Gaussian noise. The detector with threshold Θ after the observation of the transition probabilities decides which bit was transmitted with average probability of error P_e or average probability of detection P_d.

The detector employes a decision rule by which if the signal is greater than the threshold Θ, it declares messgae S_1 was transmitted,otherwise S_0 with certain probability of error.

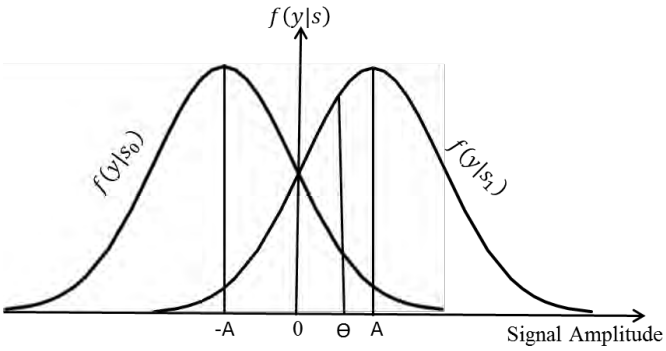

Figure 12: (2, 2) DMC with simple detection employed.

The average probability of error of the (2, 2) DMC can be evaluated using the concept of probabilities of detection and false alarm as such:

$P(e|S_0)$= $P_r(Y > \Theta)$ =the probability of error associated with bit 0

Using (10) and (11), the probability that we declare a target is present when in fact is not present is given

$$P(e|S_{0=}) = P_{fa} = \int_{\Theta}^{\infty} \frac{1}{\sqrt{2\pi\sigma^2}} \times e^{\frac{-(y+A)^2}{2\sigma^2}} dy \tag{13}$$

For a Gaussian random variable, $N\sim(\mu, \sigma^2)$, a simple change of variable in the integral in order to compute $P_r(Y > y)$, results in

$$P_r(Y > y) = Q\left(\frac{y-\mu}{\sigma}\right) \tag{14}$$

Where $Q(x)$is the error function defined as

$$Q(x) = \int_{x}^{\infty} \frac{1}{\sqrt{2\pi}} \times e^{\frac{-x^2}{2}} dx \tag{15}$$

As the $Q(x)$ is symmetric, the following relationships can be also defined mathematically

$$Q(-x) = 1 - Q(x), \qquad Q(x_1) - Q(x_2) = \int_{x_1}^{x_2} \frac{1}{\sqrt{2\pi}} \times e^{\frac{-x^2}{2}} dx \tag{16}$$

Using (14), the probability of false alarm is given

$$P(e|S_0) = Q\left(\frac{\Theta - A_0}{\sigma}\right) \tag{17}$$

Similarly the probability that we miss a target when it is in fact present, $P(e|S_1) = P_r(Y < \Theta)$ =the probability of error associated with bit 1.

Using (9) and (14), the probability of miss is given by

$$P(e|S_1) = 1 - Q\left(\frac{\Theta - A_1}{\sigma}\right) \quad (18)$$

The average probability of error as a function of the threshold Θ can be expressed [18]

$$P(e|\Theta) = p_0 \times P(e|S_0) + p_1 \times P(e|S_1) \quad (19)$$

where p_0 & $p_1$the prior probability of the bit 0 and 1 respectively

Thus,

$$P(e|\Theta) = p_0 \times Q\left(\frac{\Theta - A_0}{\sigma}\right) + p_1 \times \left(1 - Q\left(\frac{\Theta - A_1}{\sigma}\right)\right) \quad (20)$$

Average probability of detection, $P(d|\Theta) = 1 - \left[p_0 \times Q\left(\frac{\Theta - A_0}{\sigma}\right) + p_1 \times \left(1 - Q\left(\frac{\Theta - A_1}{\sigma}\right)\right)\right]$ (20.1)

The average probability of error is a function of signal amplitude, the decision threshold Θ and the noise power σ.

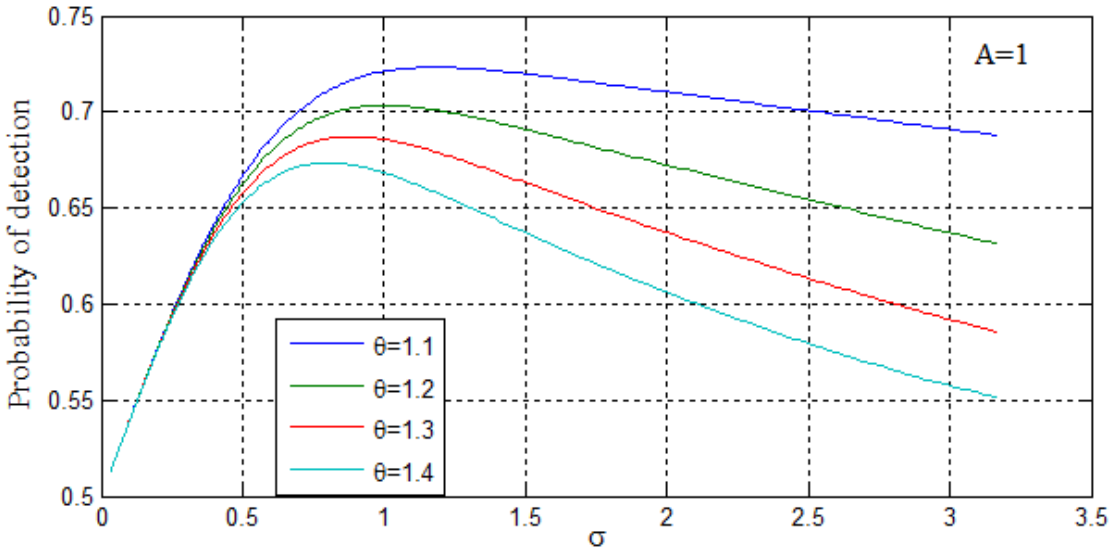

Figure 13: Probability of detection vs σ.

As shown in the Figures 13-14 using (20.1) and (20), at the optimum value of the noise power σ, the detector exhibits few errors as the probability of correct detection is maximized. A further increase of the noise power beyond that optimum value of noise deteriorates the detection performance of the receiver in line with common sense.

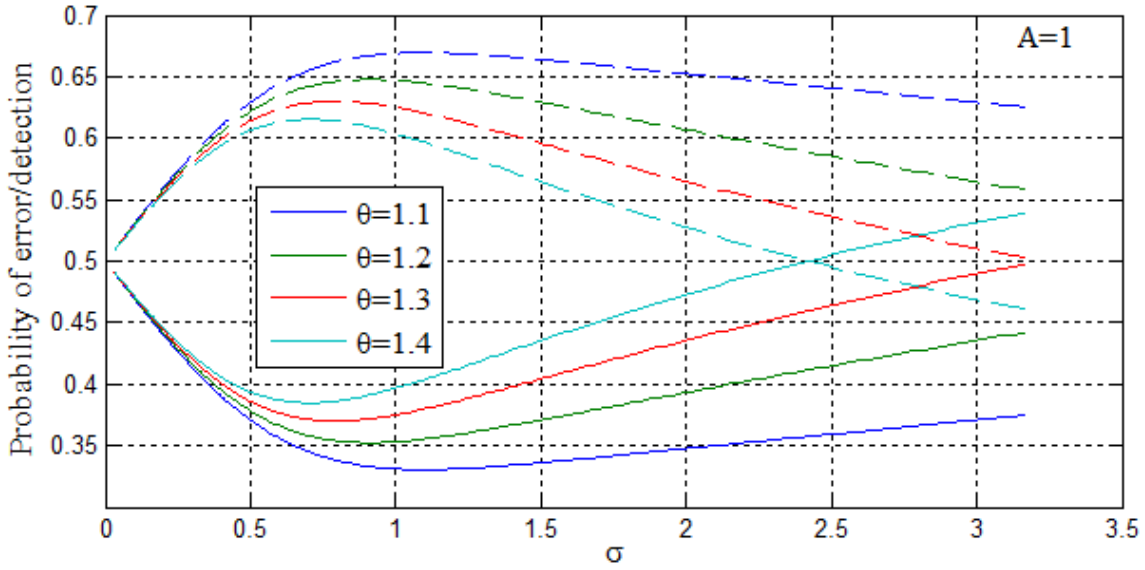

Figure 14: (2, 2) DMC performance with the AWGN. The solid and dotted lines represent the average probabilities of detection and error, respectively.

Beyond the optimum value σ, the performance of the (2, 2) DMC as shown in Figure 14 deteriorates and the addition of noise becomes disadvantageous. It is important to note that, as the decision threshold Θ increase far away from the signal amplitude *A* the performance of the detector decreases. Increasing the decision threshold from 1.1 to 1.3 for instance as shown in the Figure 13, there is a remarkable increase in the average probability of error at the crossing of the optimum noise power, sigma. Thus, the optimum value of the noise power σ is also a function of the threshold Θ for optimum system performance.

2.9 Stochastic Resonance

In general, the SR phenomenon is a non-linear effect where in communication systems the transmission of the information is enhanced in the presence of the additive noise [5]. Various performance metrics in the presence of SR such as signal to noise ratio, mutual information, and channel capacity improvement, under a certain range of power noise levels, were discussed in [3], [5],[7],[8] and [13]. In Figure 15, the average probability of error is plotted as a function of the noise power level. It is observed that the average probability of error decreases, as the noise level increases, until the detection performance reaches a resonance peak. This decrease in the probability of error is not in line with the common intuition that increasing the noise power level increases probability of error.

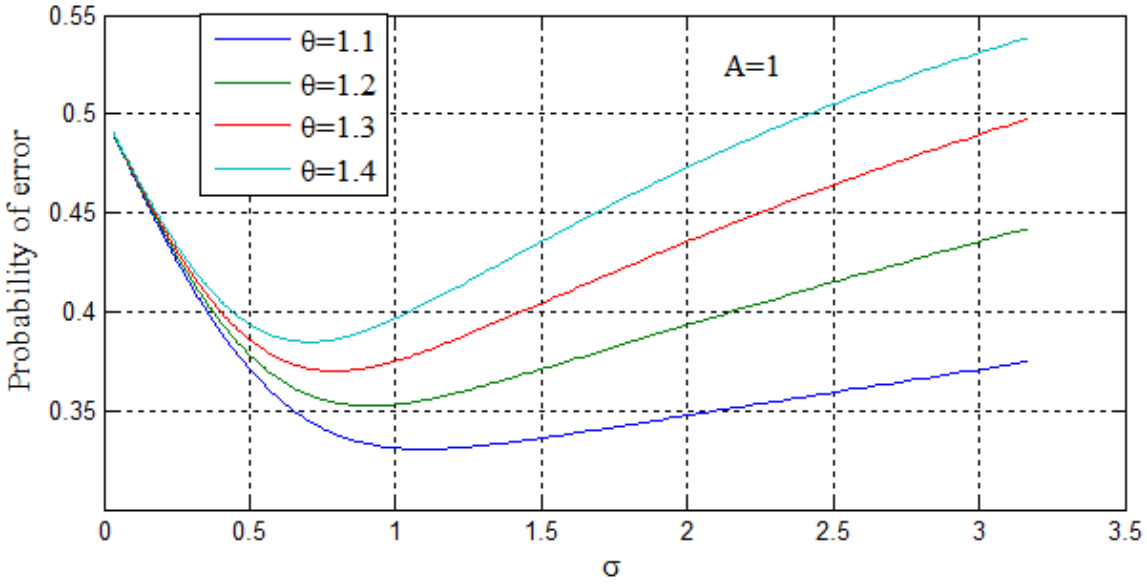

Figure 15: Probability of error in (2, 2) DMC.

In this chapter, we gave back ground review on concepts used throughout the thesis. Under Water Channel, Probability of Error, Threshold Devices, Discrete Memoryless Channels are reviewed. We also modeled the average probability of error in the (2, 2) DMC as Q function. Utilizing this analytic relationship, we discussed the performance of the (2, 2) DMC in the presence of additive Gaussian noise. Finally we discussed Stochastic Resonance effect in nonlinear systems, in particular in the case of the (2, 2) DMC.

Chapter 3

(2, 3) DMC and Probability of Error

In this chapter, we focus on the general (2, 3) DMC and its particular case, the (2, 2) binary asymmetric channel. In Section 3.2, we derive the average probability of error for the (2, 3) DMC.

3.1 The (2, 3) DMC

The (2, 3) DMC $\{M: X \to Y\}$ is characterized by a binary input random variable $X = \{1, -1\}$, a ternary output random variable $Y = \{1,0, -1\}$ and a transition probability matrix, M, [5].

$$M = \begin{pmatrix} P_{11} & P_{21} & P_{31} \\ P_{12} & P_{22} & P_{32} \end{pmatrix}$$

where P_{ji}, is the probability of receiving signal j given signal i was transmitted. The transition probability matrix from X to Y is given by

$$P_{11} = P(Y = 1|X = 1)\ ,P_{21} = P(Y = 0|X = 1),P_{31} = P(Y = -1|X = 1)$$

$$P_{12} = P(Y = 1|X = -1),P_{22} = P(Y = 0|X = -1),P_{32} = P(Y = -1|X = 1)$$

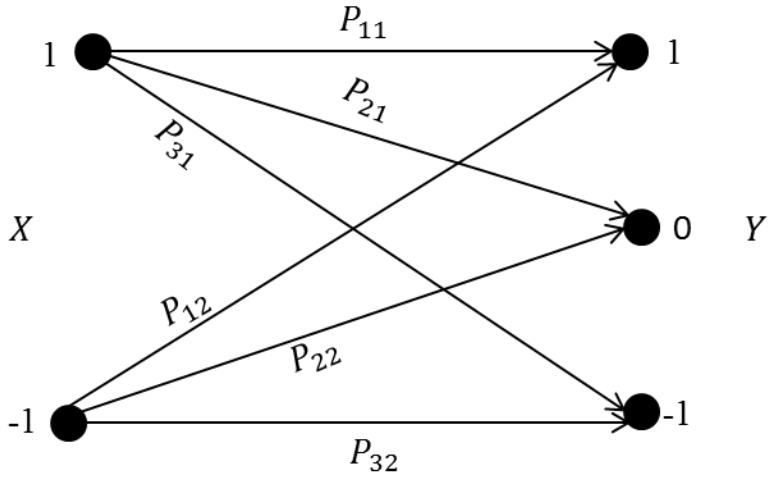

Figure 16: (2, 3) DMC representation.

The input to the threshold communication channel is the signal that takes the binary values ±A as in [5], with probability p_0 and p_1. The physical model is represented in Figure 16.The (2, 3) DMC detector transforms the observation into a value which is finally compared to a threshold Θ to make a decision.

.

3.2 System Model

The input to the threshold communication channel is the signal that takes the binary values ±A as in [5], [14] with probability p_0 and p_1. The physical model is represented in Figure 17. The (2, 3) DMC detector transforms the observation into a value which is finally compared to a threshold Θ to make a decision. The DMC is completely characterized by the transition probabilities of the output conditioned by the input probabilities.

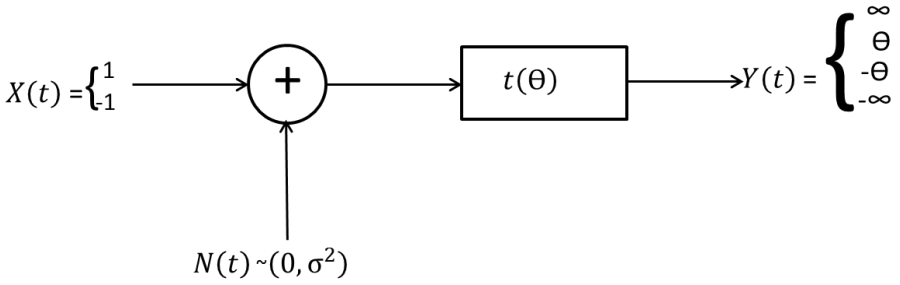

Figure 17: System model of (2, 3) DMC.

The physical communication channel contains a threshold decision block function threshold $t(\Theta)$, where $t(\Theta)$ represents the threshold value. Based on the threshold level Θ and the noise level, the received signal is converted into a discrete random variable $Y(t)$ taking on the values of 1, 0, or -1. We assumed antipodal signaling and a new symmetric decision threshold was defined around the optimum threshold in the (2, 2) DMC which gave rise into three distinct regions at the output as shown in figure above.

Adapting the model of [5], we first defined four different regions of interest. These are C_0, C_1, D_0 and D_1 as shown in Figure 18. We incorporated the (2, 2) and the classical simple (2, 3) DMCs optimum detection schemes to study the effect of additive Gaussian noise in the case of our modified (2, 3) DMC. The (2, 2) and (2, 3) DMCs are represented with zero detection threshold and symmetric threshold Θ respectively.

Finally we derived the analytic relationship for the probability of error in the (2, 3) DMC. We investigated the effect of AWGN on the probability of error of the (2, 3) DMC for different value of decision threshold Θ and noise power σ.

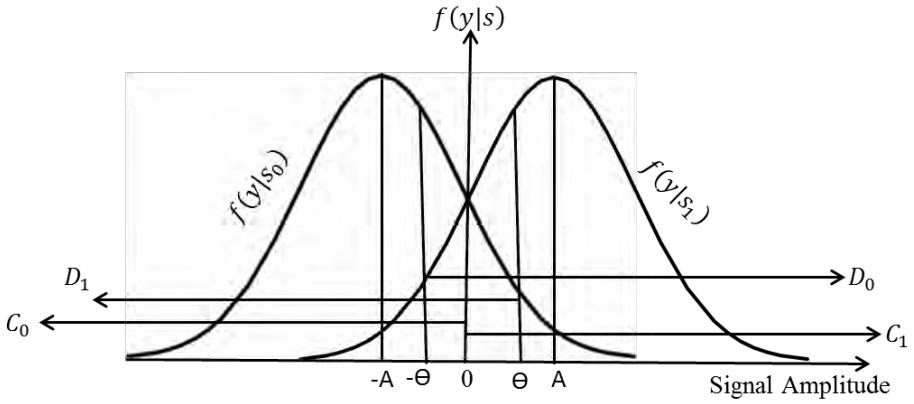

Figure 18: Regions of interest in the (2, 3) DMC. Bit 0 and 1 are represented by voltage waveforms S_0 and S_1 respectively. A is the signal amplitude and Θ our symmetric decision threshold.

We defined probability of miss as the conditional probability that the received signal is less than the threshold Θ given it is greater than the zero optimum threshold in the (2, 2) DMC. Similarly the probability of false alarm is the conditional probability that the received signal is greater than the symmetric negative threshold theta given that the received signal is less than the optimum threshold Θ in the (2, 2) DMC. Thus, we have the following relations.

$$\mathrm{P}(e|S_1) = \mathrm{P}(D_1|C_1) = \frac{P(C_1 \cap D_1)}{P(C_1)} \tag{21}$$

where D_1 is the region for which the conditional probability $f(y|S_1)$ is less than the threshold Θ as shown in Figure 18. Also C_1 is the region for which the conditional probability $f(y|S_1)$ is greater than the zero decision threshold as shown in figure above.

These two areas are intersecting in a certain fashion as follows:

$$P(C_1 \cap D_1) = \int_0^{\Theta} f(y|S_1)\, dy \tag{22}$$

Using (8), (14), and (15), the area of intersection can be modeled as Q function

$$P(C_1 \cap D_1) = 1 - Q\left(\frac{A}{\sigma}\right) - Q\left(\frac{\Theta - A}{\sigma}\right) \tag{23}$$

The detector correctly decodes the bit 1 if it receives a voltage greater than zero in the (2, 2) DMC. Therefore,

$$P(C_1) = \int_0^{\infty} f(y)dy \tag{24}$$

Substituting (8) and (14), we obtain

$$\mathrm{P}(C_1) = 1 - Q\left(\frac{A}{\sigma}\right) \tag{25}$$

Combining (22) and (25) we will get

$$P(e|S_1) = \frac{1-Q\left(\frac{A}{\sigma}\right) - Q\left(\frac{\theta-A}{\sigma}\right)}{1-Q\left(\frac{A}{\sigma}\right)} \tag{26}$$

Following similar argument the probability that is associated with bit zero can be calculated as follows

$$\mathrm{P}(e|S_0) = \mathrm{P}(D_0|C_0) = \frac{\mathrm{P}(C_0 \cap D_0)}{\mathrm{P}(C_0)} \tag{27}$$

where D_0 is the region for which the conditional probability $f(y|S_0)$ is greater than the –Θ threshold as shown in Figure 18. Also C_0 is the region for which the conditional probability $f(y|S_0)$ is less than the zero decision threshold .

The area for which these parameters of interest are overlapping can be summarized as follows:

$$P(C_0 \cap D_0) = \int_{-\theta}^{0} f(y|S_0)\, dy \tag{28}$$

Employing (8), (14), and (15) we will obtain

$$P(C_0 \cap D_0) = Q\left(\frac{A-\theta}{\sigma}\right) - Q\left(\frac{A}{\sigma}\right) \tag{29}$$

Also a simple (2, 2) DMC decodes the bit zero, when the voltage received is less than the reference zero voltage.

Therefore,

$$P(C_0) = \int_{-\infty}^{0} f(y|S_0)dy \tag{30}$$

Using (8), (14), and (15) we will obtain

$$P(C_0) = 1 - Q\left(\frac{A}{\sigma}\right) \tag{31}$$

Combining (28) and (30), we get the probability of false alarm that the detector declares a target is present when in fact is missing is represented by the following Q function

$$P(e|S_0) = \frac{Q\left(\frac{A-\theta}{\sigma}\right) - Q\left(\frac{A}{\sigma}\right)}{1-Q\left(\frac{A}{\sigma}\right)} \tag{32}$$

Using (19) the average probability of error for the (2, 3) DMC which analytically incorporates the optimum detection threshold of the (2, 2) DMC, will be calculated as such

$$P(e|\Theta) = p_0 \times \frac{\boldsymbol{Q\left(\frac{A-\Theta}{\sigma}\right)}}{\boldsymbol{1-Q\left(\frac{A}{\sigma}\right)}} + p_1 \times \frac{1-Q\left(\frac{A}{\sigma}\right)- Q\left(\frac{\Theta-A}{\sigma}\right)}{1-Q\left(\frac{A}{\sigma}\right)} \tag{33}$$

Since probability of error and detection add up to 1. We get,

$$P(d|\Theta) = 1 - \left[p_0 \times \frac{\boldsymbol{Q\left(\frac{A-\Theta}{\sigma}\right)}}{\boldsymbol{1-Q\left(\frac{A}{\sigma}\right)}} + p_1 \times \frac{1-Q\left(\frac{A}{\sigma}\right)- Q\left(\frac{\Theta-A}{\sigma}\right)}{1-Q\left(\frac{A}{\sigma}\right)}\right] \tag{33.1}$$

where p_0 and p_1 are the prior probabilities of bit 0 and 1 respectively and $P(d)$ is probability of detection.

As the classical probability of error curves are plotted with respect to the signal to noise ratio (γ), we also remodeled our average probability of error for the (2, 3) DMC by letting $\frac{A}{\sigma} = \sqrt{\gamma}$. By doing so, we were able to compare (32) with conventional probability of error curves and deduce the location of our symmetric decision threshold relative to the signal amplitude.

$$P(e|\Theta) = p_0 \times \frac{Q\left(\sqrt{\gamma}\left(1-\frac{\Theta}{A}\right)\right)-Q(\sqrt{\gamma})}{1-Q(\sqrt{\gamma})} + p_1 \times \frac{1-Q(\sqrt{\gamma})\left(\frac{\Theta}{A}-1\right)-Q(\sqrt{\gamma})}{1-Q(\sqrt{\gamma})} \tag{34.1}$$

As (33) shows the average probability of error is a function of signal amplitude, noise intensity and decision threshold Θ. Using this analytic relationship we studied how the probability of error varies as a function of signal to noise ratio γ by either varying the signal amplitude and fixing the threshold or vice versa. We examined how the amplitude of the signal is related to the decision threshold Θ by plotting the probability of error curves as a function of γ as shown in Figures 19-20.

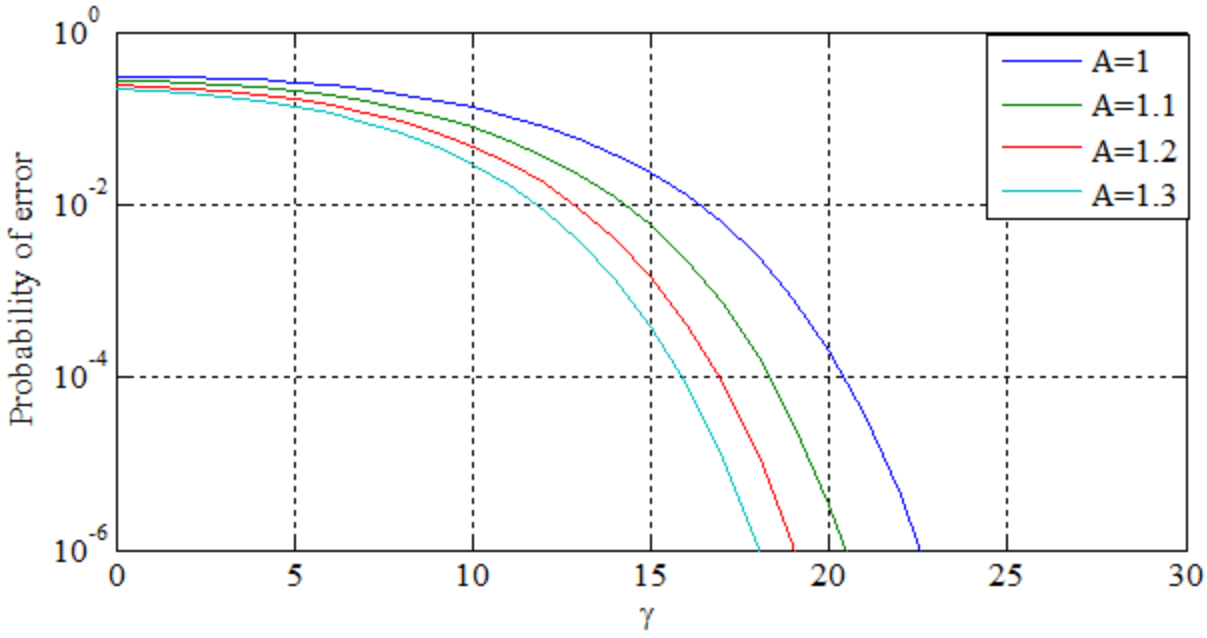

Figure 19: Probability of error vs γ when Θ is 0.75.

In order to achieve the same probability of error by either fixing the threshold or the signal amplitude, one needs to increase the γ to compensate the decrease in the Euclidian distance between the threshold and signal amplitude as shown in the Figure above. Alternatively speaking for the same γ the probability of error increase as the threshold approaches the amplitude of the signal.

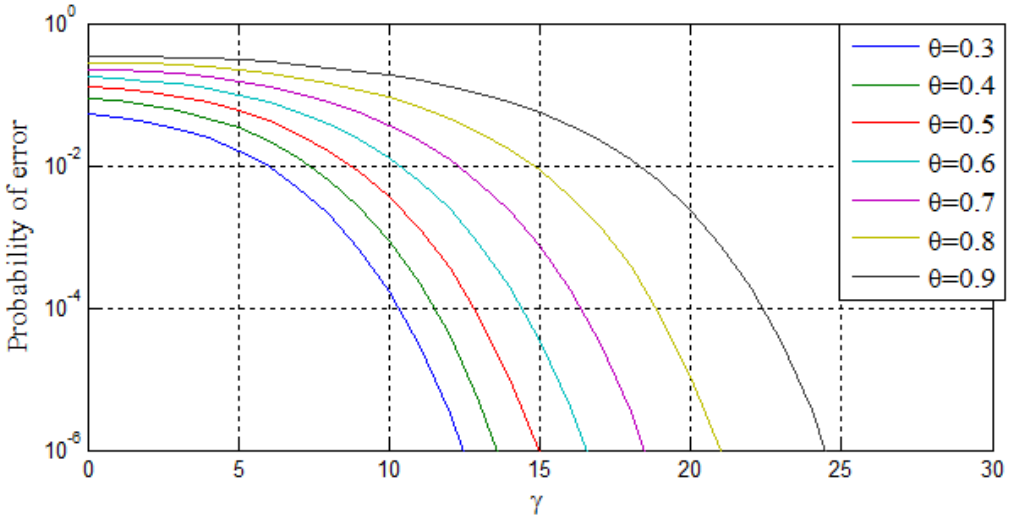

Figure 20: Probability of error vs γ for signal amplitude, A=1.

As shown in Figure 20, for the same γ, the probability of error increases as the detection threshold Θ increases and approaches our signal amplitude (A=1). For the same value of Θ, the probability of error decreases as the γ increases.

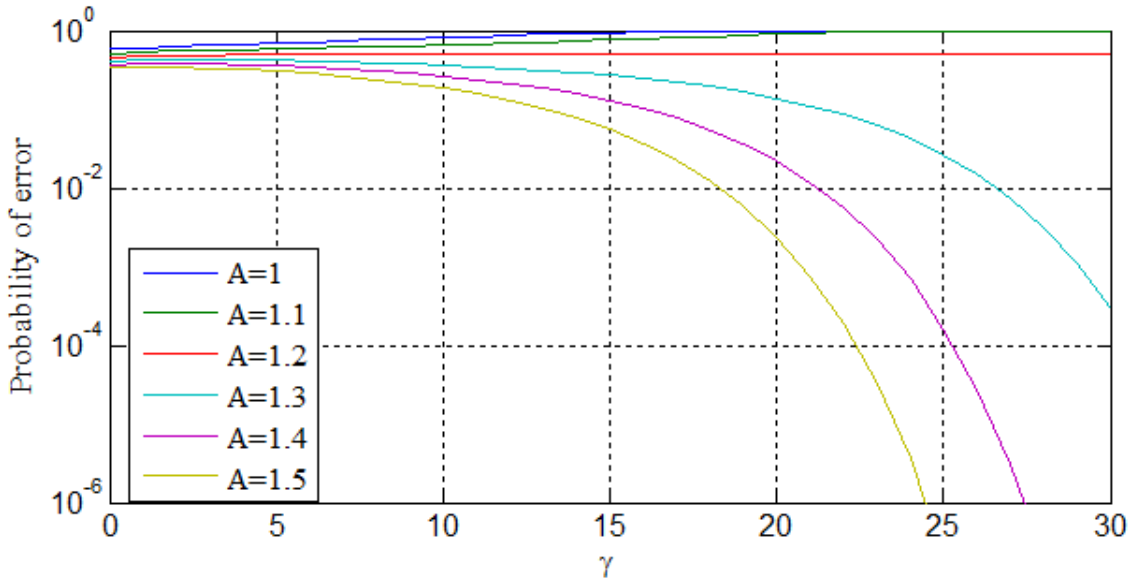

Figure 21: Probability of error for the (2, 3) DMC vs γ for Θ=1.2.

However, if threshold becomes ≥ the amplitude of the signal as shown in the Figure 21, then we end up of making a total error, i.e. for A=1 and 1.1 in figure above. Thus, to achieve a minimum probability of error, the threshold Θ should be less than our signal amplitude in our modified (2, 3) DMC, i.e $0<\Theta<A$.

Alternatively, if we increase the Euclidian distance between the signal amplitude and the threshold beyond a certain limit, i.e. $A> \Theta$ the probability of error curves become close and fall sharply. The minimum attainable probability of error is obtained at lower γ.

.

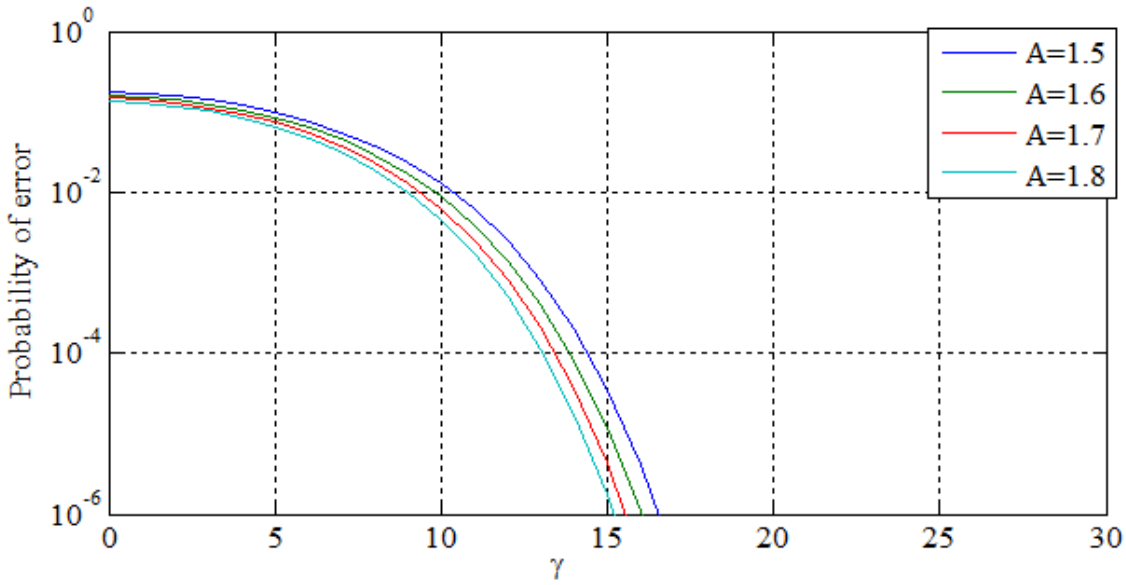

Figure 22: Probability of error for the (2, 3) DMC as a function of γ for Θ=0.75.

As depict in figure above, as our detection threshold theta approximately becomes$< \left(\frac{A}{2}\right)$, the probability of error curves decay so fast compared to Figure 20-21. Also for the same γ, the probability of detection gain among the different signaling scenarios become negligible.

After studying the effect of the relative Euclidian distances between the signal amplitude and the detection threshold Θ on the average probability of error in our modified (2, 3) DMC, we proceed our investigations to study the effect of the above observed dependencies considering probabilities of true detection, false alarm, miss and rejection in the modified (2, 3) DMC.

Probability of false alarm in the modified (2, 3) DMC is nothing but $P(e|S_0)$. Since probability of false alarm and rejection add up into one, using (32) we get (34.2) as follows:

$$P(e|S_0) = P_{fa} = \frac{Q\left(\frac{A-\Theta}{\sigma}\right)-Q\left(\frac{A}{\sigma}\right)}{1-Q\left(\frac{A}{\sigma}\right)}, \text{ and } \quad P_r = 1 - \frac{Q\left(\frac{A-\Theta}{\sigma}\right)-Q\left(\frac{A}{\sigma}\right)}{1-Q\left(\frac{A}{\sigma}\right)} \tag{34.2}$$

where P_{fa} and P_r are the probabilities of false alarm and rejection respectively.

Similarly as the probability of miss and true detection sum up into one. Utilizing the fact that the probability of miss is equivalent to $P(e|S_1)$, we arrived at (34.3) as follows:

$$P(e|S_1) = P_m = \frac{1-Q\left(\frac{A}{\sigma}\right)- Q\left(\frac{\Theta-A}{\sigma}\right)}{1-Q\left(\frac{A}{\sigma}\right)} \text{ , and } \quad P_{dt} = 1 - \frac{1-Q\left(\frac{A}{\sigma}\right)- Q\left(\frac{\Theta-A}{\sigma}\right)}{1-Q\left(\frac{A}{\sigma}\right)} \tag{34.3}$$

where P_m and P_{dt} are the probabilities of miss and true detection respectively.

Using (34.2) and (34.3) as shown in Figures 23-27, we studied how the selection of the threshold Θ, the signal amplitude and the noise power determine these above probabilities of interest.

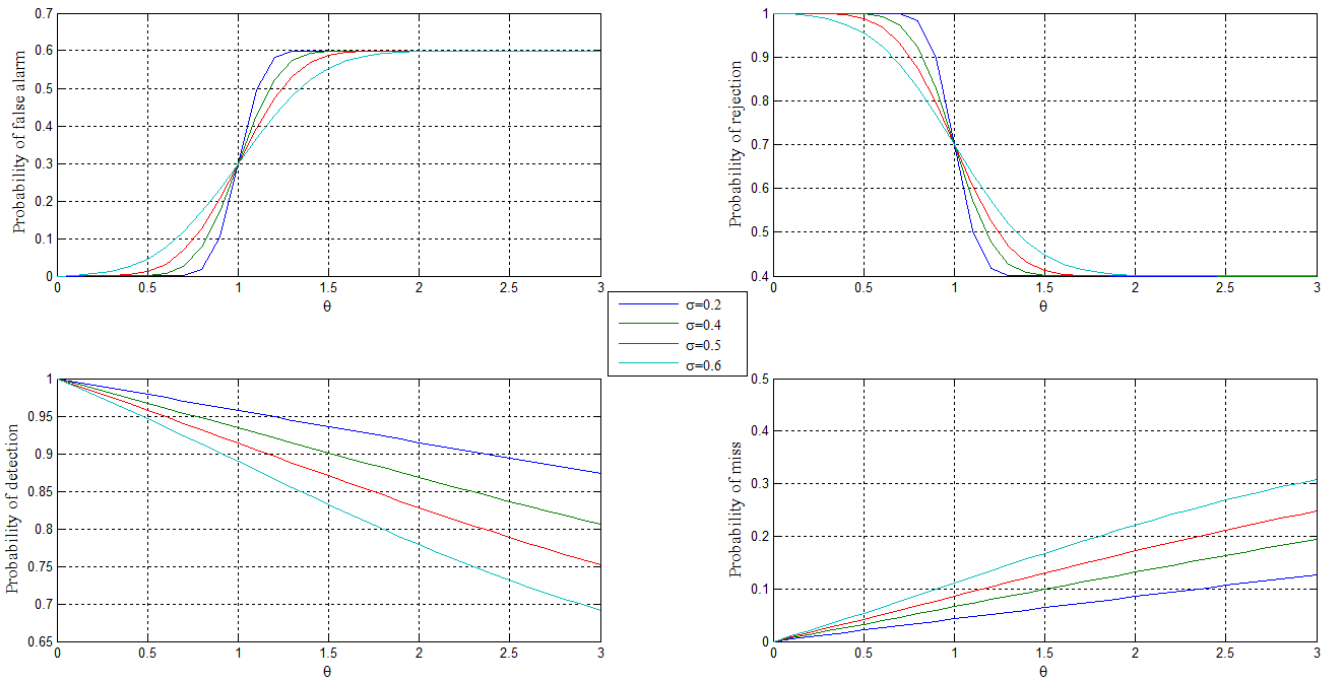

Figure 23: Probabilities of error vs Θ. The signal amplitude is 1.

The selection of the decision threshold Θ, not only affects the average probability of error but also the probabilities of false alarm, true detection, miss and rejection. Analytic relationships (33.2) and (33.3) are used to study the above mentioned probabilities. As the threshold Θ increases towards the signal amplitude, as shown in the Figure 23, the probabilities of false alarm and miss increase. Also the probabilities of true detection and rejection sharply decrease with increase of Θ. After observing the effect of Θ on the above mentioned probabilities, we conducted similar investigations by corresponding each of the probabilities against the other as shown in Figures 24-27, for the signal amplitude (A=1).

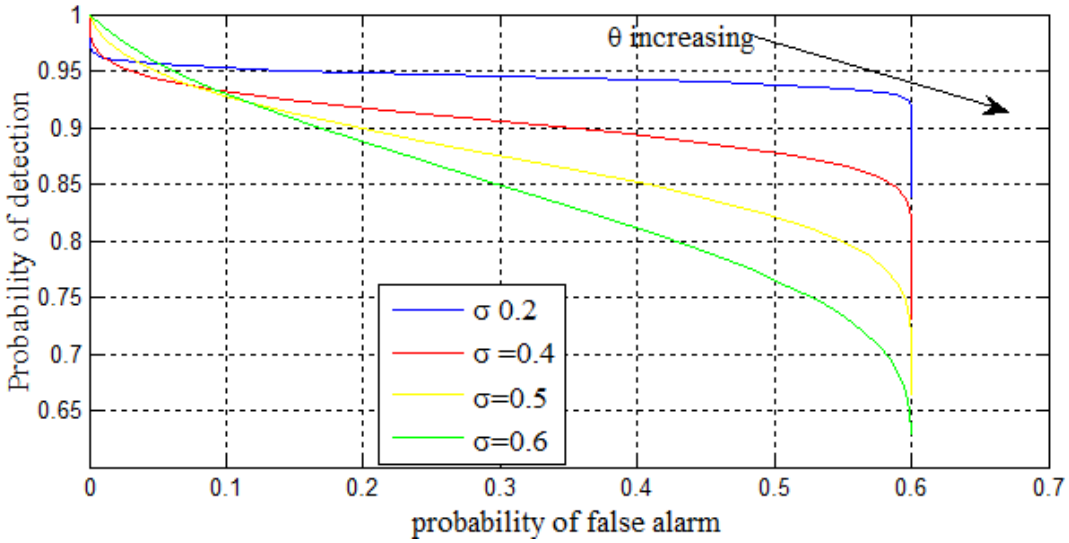

Figure 24: Probability of true detection vs probability of false alarm.

Figure 24 represents receiver operating characteristics curves in the case of our modified (2, 3) DMC, for fixed value of the noise powers σ as the decision threshold Θ increases from zero. As the decision threshold Θ increases the probability of true detection decreases. As the decision threshold is symmetric, positive increase of Θ is also manifested in the increase of the negative threshold Θ, thus the probability of false alarm is also increased. The probability of false alarm curves reaches a maximum (0.6) value as shown in the figure above.

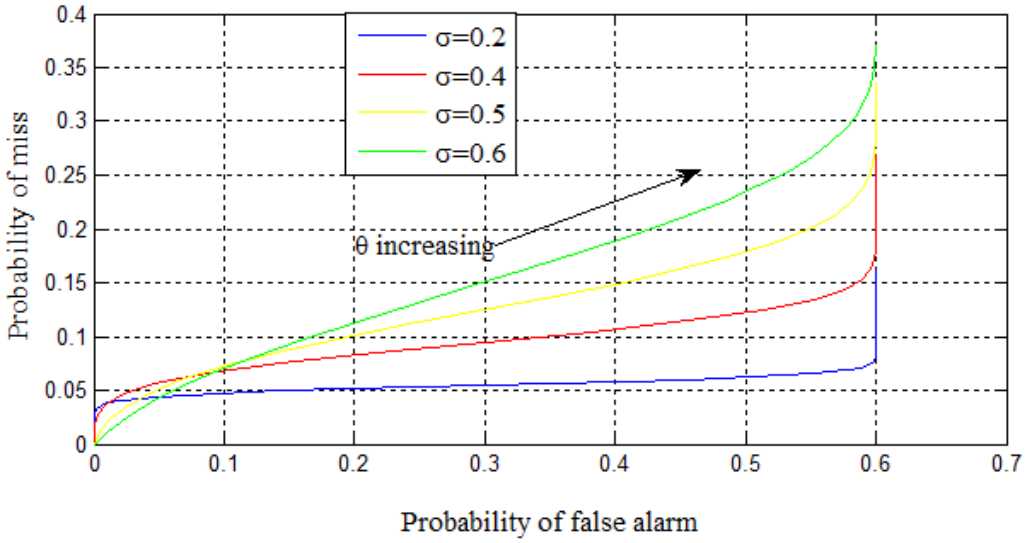

Figure 25: Probability of miss vs probability false alarm.

The decrease of the probability of detection with increase of the threshold is verified with the increase of the probability of miss as shown in the Figure 25 by using (33.2-3). For optimum system performance we need to have a detector which minimizes both probability of miss and false alarm.

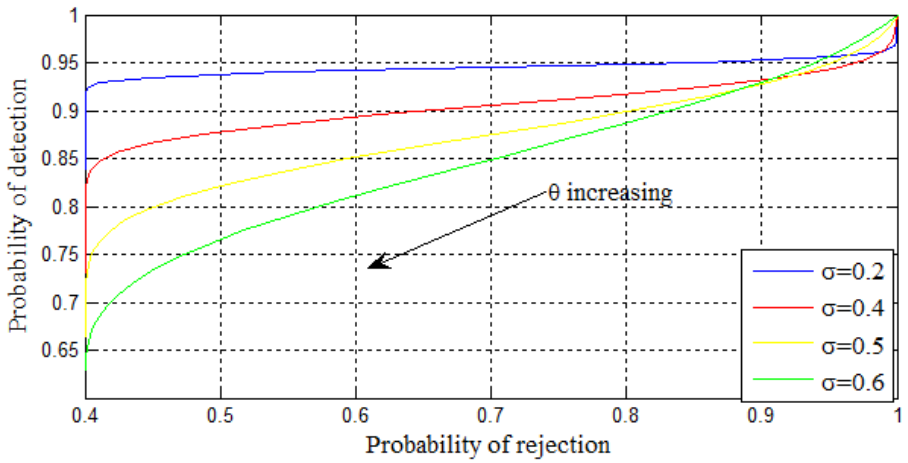

Figure 26: Probability of detection vs probability of rejection.

A conservative detection is achieved by maximizing the probabilities of true detection and rejection. As depicted in Figure 26, increasing the threshold Θ results in a liberal system for which our detection performance decrease as more and more false alarms are generated. However, as the decision threshold Θ regresses towards the (2, 2) DMC optimum threshold, probability of true detection is maximized, as the system blocks the false alarm by maximizing the probability of rejection.

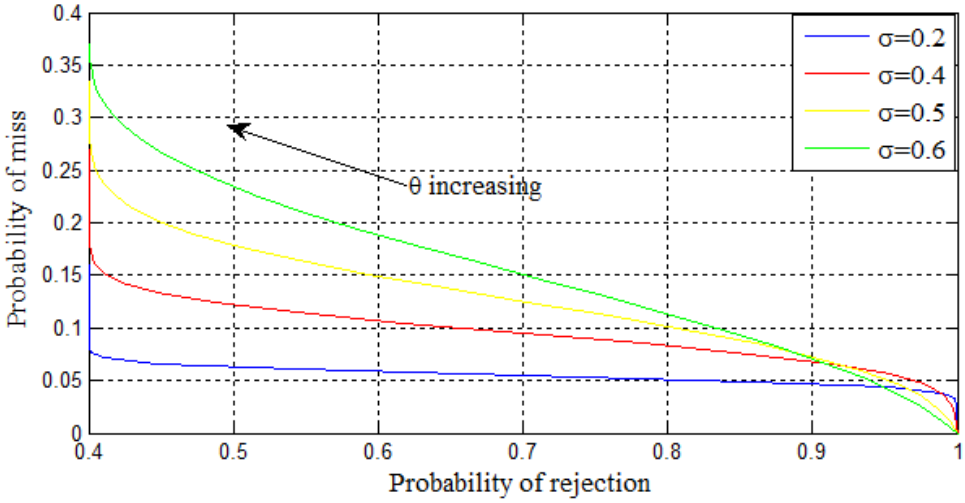

Figure 27: Probability of miss vs probability rejection.

For better target detection and tracking, we need to minimize the probability that we miss a target by maximizing our detection. At the same time the false alarm that is generated should be minimized by maximizing the probability of declaring there is no target in the absence of a valid target. As it is depicted above, as the decision threshold theta exceeds our signal amplitude, the probability that we miss a valid target increases. Similarly, the detector generates a lot of false alarms limiting the capability of rejecting a target when it is absent.

Summing up, in Chapter 3 we first incorporated the (2, 2) and the simple (2, 3) DMCs optimum detection schemes in the study of the modified (2, 3) DMC. We then derived the analytical relationship that relates the average probability of error as a function of the signal amplitude, detection threshold Θ and noise power σ. We studied the trade-off between the signal amplitude and threshold Θ for better target detection and tracking. We investigated how the average probability of error curve behaves in the case of sub/suprathreshold signaling. We deduced the interval by which the symmetric threshold Θ needs to be located relative to the signal amplitude A for optimum system performance in the presence of additive Gaussian noise. Moreover, we classified the average probability of error into the probabilities of false alarm, true detection, miss and rejection to study and investigate the effect of the placement of Θ relative to the signal amplitude. Furthermore, we studied these four probabilities against each other and observed similar patterns as in the case of the average probability of error. These above mentioned results and observations will be utilized in Chapter 4 to investigate the SR effect in the (2, 3) DMC.

Chapter 4

Principles and System Model of Stochastic Resonance (SR)

SR is a phenomenon where the presence of internal or external input noise in non- linear systems provides a better system response to the input signal than in the absence of noise. SR doesn't occur in linear systems. Thus for SR to occur three basic ingredients [20] as shown in Figure 28, are required, namely:

- Sub/superthreshold input signal $X(t)$
- A source of noise which could be either inherent in the systems or that adds to the coherent input $N(t)$
- Nonlinear activation barrier or a form of threshold Θ

4.1 System Model of Stochastic Resonance (SR)

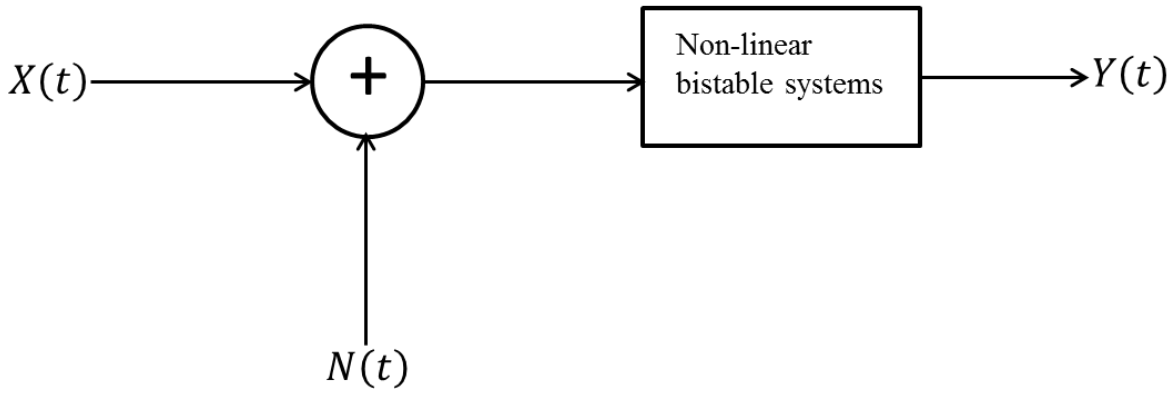

Figure 28: System Model of SR. The noise variable $N(\boldsymbol{t})$ is ~ $(0,\sigma^{\boldsymbol{2}})$, $Y(t)$ is the response of the bistable system.

If the above conditions are met then the system undergoes resonance- kind of behavior as a function of noise level. SR has been observed in a large variety of systems, including schmit trigger electronic circuits, bidirectional ring lasers and cray fish mechanoreceptors [3],[9],[11],[13].

The counterintuitive effect relies in systems non linearity and some parameter ranges being 'suboptimal'. Stochastic resonance has been observed, quantified and described a plethora of physical and biological systems, including neurons,[8],[12]. Being a topic of widespread multidisciplinary interest, the definition of stochastic resonance has evolved significantly over the last decade or so, leading to a number of debates, misunderstandings and controversies.

Using (33.1) the probability of correct detection is plotted as a function of the noise power level as shown in Figure 31 . It is observed that the probability of detection increases as the noise level increases, until the probability of detection reaches a resonance maximum.This increase in probability of correct detection is not in accordance with the intuition that increasing the noise power level will decrease the probability of correct detection.

In [10] and [11], the SR effect is observed on the binary-input binary-output (2,2) DMC Probability of error, where minimum probability of error occurs at an optimal power σ of the additive Gaussian noise(AGN) in relation to a given threshold level , as depicted in Figure 15.

4.2 Sub/ Superthreshold input signal

In this thesis, following Ira Moskovitz work in [6], we analyzed the physical communication model of the (2,3) DMC for threshold based SR due to additive noise. We defined symmetric decision threshold as shown in Figure 18 and by conditioning the probability of false alarm and miss to the optimum regions in the (2, 2) DMC, the average probability of error as a function of the decision threshold theta, noise power sigma and signal amplitude is analyzed for better system performance in the presence of additive guassian noise.

In Chapter 3, we investigated the average probabiltiy of error curves in the context of the modified (2, 3) DMC. We fixed the amplitude of the signal and by varying the signal to noise ratio, we examined the relationship between the detection threshold Θ and the signal amplitude. However, to study the effect of SR in the modified (2, 3) DMC, we need to examine the average probability of error or probability of detection relative to the noise power by fixing the signal amplitude.

In order to investigate the effect of suprathreshold barrier ($\Theta > A$), we generated Figure 29 using (33.1). As the detection Θ is greater than the signal amplitude, there exist no noise enhanced signal detection. The detection performance of the detector deteriorates as the noise power σ increases. This observation is consistent with the probability of error curves that we discussed in chapter 3.

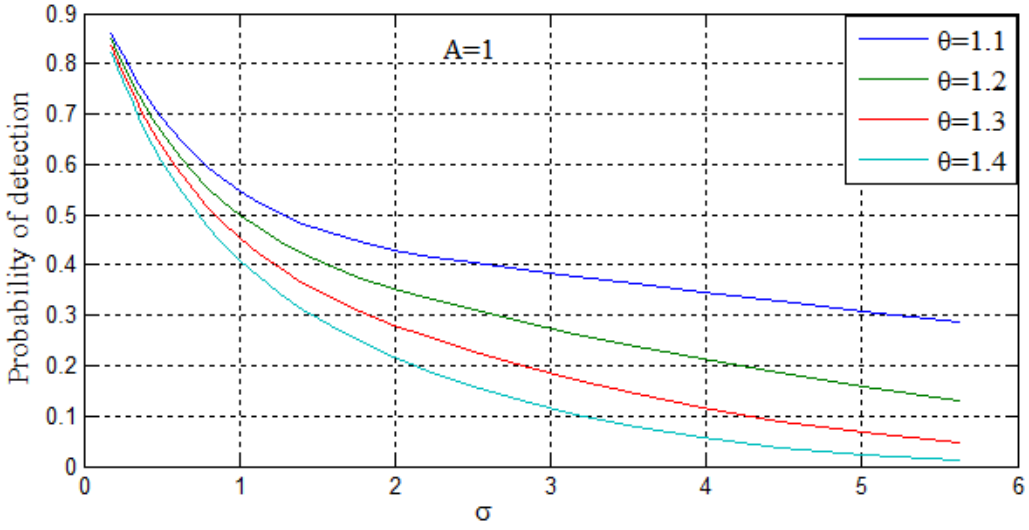

Figure 29: probability of detection in the (2, 3) DMC. The signal amplitude is 1.

As the detection threshold Θ becomes greater than the signal amplitude in the (2, 3) DMC as shown in Figure 29, there is no noise enhanced signal detection.

.

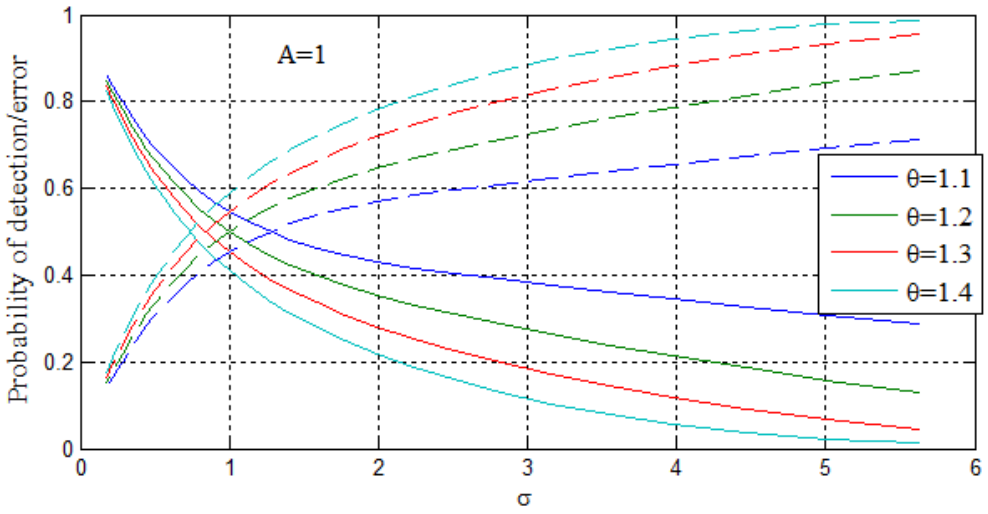

Figure 30: Performance metrics in the (2, 3) DMC. The solid line represents probability of correct detection, while the dotted line represents probability of error.

In the modified (2, 3) DMC, if the threshold Θ is greater than the signal amplitude, the probability of error increases as the noise power σ increases as shown in Figure 30. From this observation and the investigations that we did in chapter 3, we claim, the SR effect can only occur in the interval [-Θ, Θ] for which Θ< the signal amplitude A.

4.3 SR and the (2, 3) DMC

Tiny, low-power, low-cost transceiver, sensing, and processing units need to be designed for a successful deployment of underwater distributed wireless sensor networks. As target detection and tracking is essential on those distributed networks, we re-examined the (2, 3) DMC in three dimensional view to observe stochastic resonance effect. We observed the phenomenon of SR on the probability of signal detection over a specific range of Θ and noise variance σ. In Figure 31 using (33.1) we plotted probability of correct detection for different value of the threshold Θ. For a fixed threshold the performance of the detector increase until it reaches its peak value and it starts to decrease as the noise value increases beyond the optimum value. This resonant effect can be easily observed in the 3-D plot. As what it is clearly shown in the Figure 32 the signal detection reaches maximum in a range which is both dependent on the decision threshold and the noise variance. As the noise increases beyond a certain limit, the performance of the detector deteriorates and adding additional amount of noise becomes useless in accordance with common sense. However, there exists an optimum noise which gives better system performance as shown in Figure 31. In the other hand, as the decision threshold theta increase far away from our signal amplitude as shown in Figures 29-30 , the performance of the modified (2, 3) DMC deteriorates.

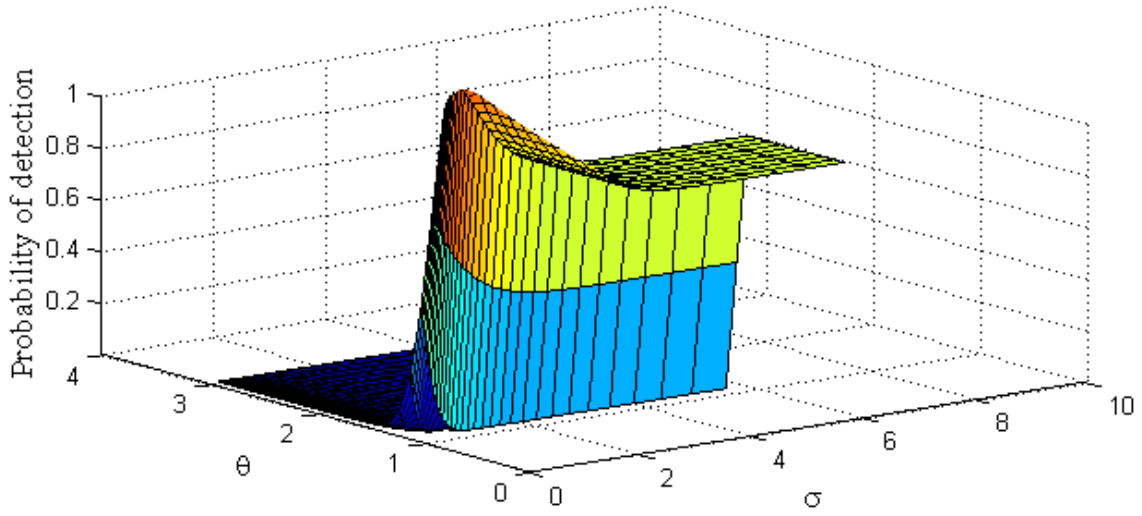

Figure 31: Probability of detection and SR in the (2, 3) DMC. The signal amplitude is 1.

In underwater distributed wireless sensor networks, signal detection and estimation problem is on how to maximize the detectability of a target by minimizing the probabilities of false alarm and miss. As depicted in Figure 32 using (33.1), the increase of the signal amplitude from A=1 to 1.2 boosts the signal detection. Thus by carefully selecting the systems parameters, in the presence of additive white Gaussian noise, one can achieve better signal detection and estimation. As we need to adhere to the power constraints that we have in case of the UWC, we can alternatively select the symmetric detection threshold Θ to maximize our target detection.

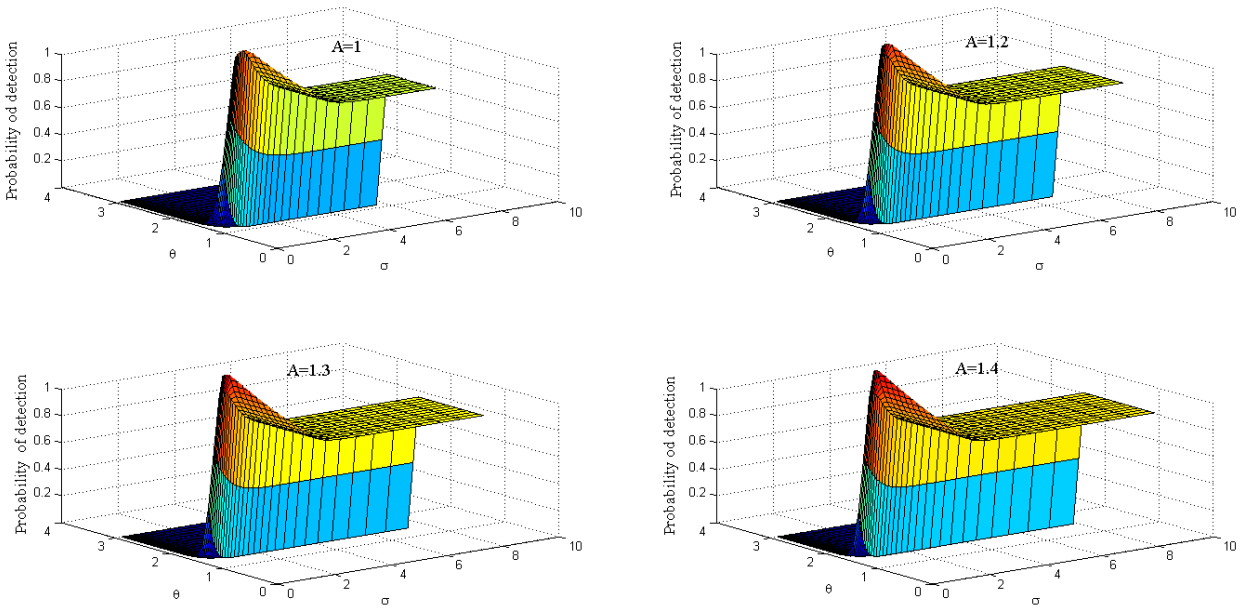

Figure 32: SR in (2, 3) DMC for different value of signal amplitude.

4.4 Performance comparison of the (2, 2) and (2, 3) DMCs

Regardless of which type of medium access scheme is used for sensor networks, it important for the detector to detect the target with less probability of error. Relationships (20) and (33.1) are used to compare the performance of the (2, 2) and the (2, 3) DMCs when the threshold Θ is greater than the signal amplitude. The (2, 2) DMC exhibits noise enhanced detection for Θ > signal amplitude as shown in the figure below. However, the performance of the (2, 3) DMC worsens. But, for Θ< the signal amplitude the performance of the modified (2, 3) DMC is much better than the (2, 2) DMC as shown in Figure 31. The probability of detection (2, 3) DMC increases when the noise power σ increases until it reaches its optimum value. Further addition of noise deteriorates the performance of the detectors and probability of detection decreases.

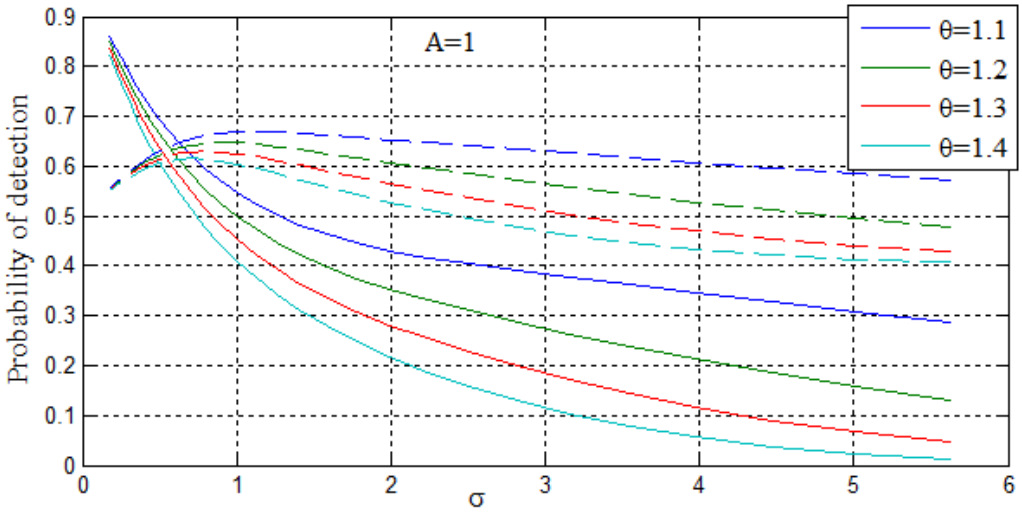

Figure 33: Probabilities of detection in the (2, 2) and (2, 3) DMCs. The solid and dotted line represent probabilities of detection in the (2 3) and (2, 2) DMCs respectively.

As the detection threshold Θ is greater than our signal amplitude, we observe noise enhanced better signal detection with less probability of error in the case of the (2, 2) DMC as shown in Figures 33-34.

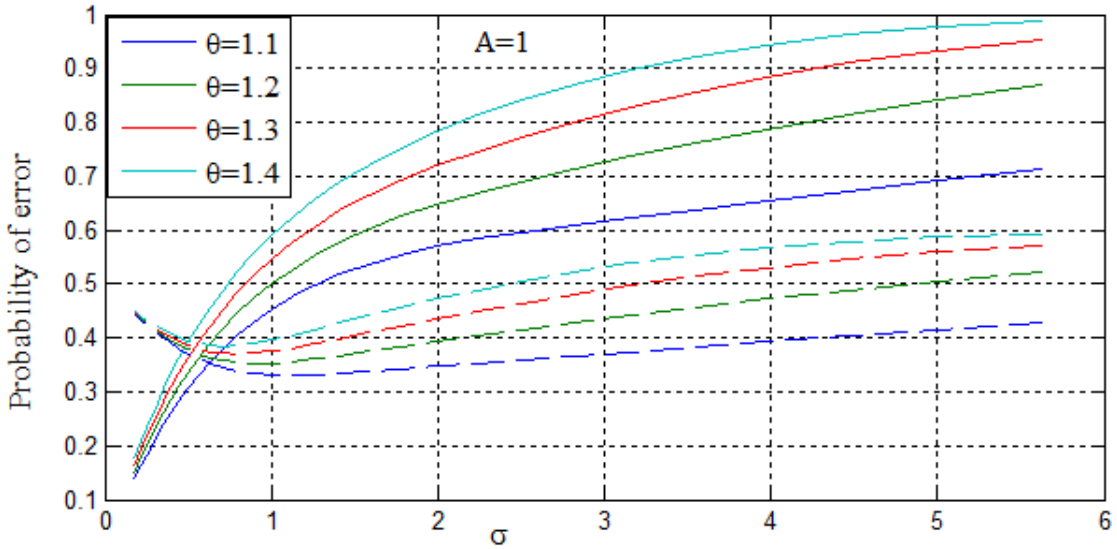

Figure 34: Probability error in the (2, 2) and (2, 3) DMCs. The solid and dotted line represent probabilities of error in the (2 3) and the (2, 2) DMCs respectively.

Another important comparison can be drawn between the two (2, 3) DMCs; the average probability of error in the simple (2, 3) DMC, can be calculated as shown in the Figure 35 as follows.

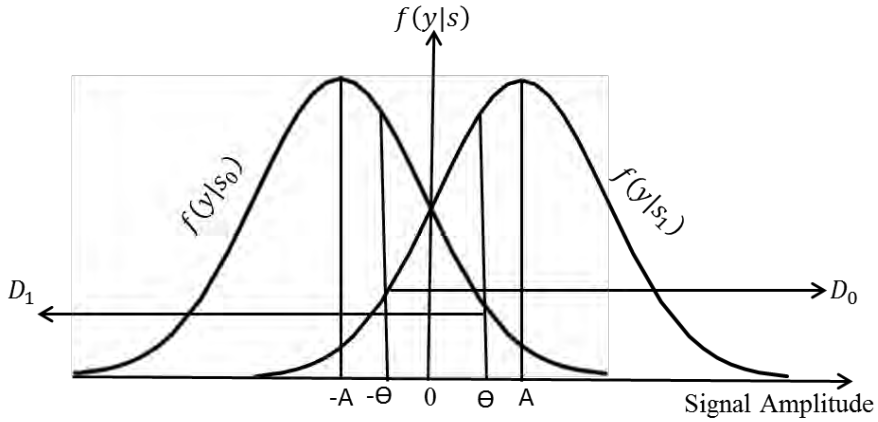

Figure 35: A simple (2, 3) DMC detection scheme. The errors associated with bit 0 and 1 are represented by the areas D_0 and D_1 respectively.

The error associated with bit 0 is the area under the pdf, $(y|S_0) > -\Theta$. Thus

$$P(e|S_1) = Q\left(\frac{-\theta - A_0}{\sigma}\right)$$

Similarly the error associated with bit 1 is the areas under the pdf, $f(y|s_1) < \Theta$.

$$P(e|S_1) = \left(1 - Q\left(\frac{\Theta - A_1}{\sigma}\right)\right)$$

Using (19), thus the average probability of error is given by

$$P(e|\Theta) = p_0 \times Q\left(\tfrac{-\Theta - A_0}{\sigma}\right) + p_1 \times \left(1 - Q\left(\tfrac{\Theta - A_1}{\sigma}\right)\right) \tag{35}$$

The average probability of detection in the simple (2, 3) DMC can be obtained as follows:

$$P(d|\Theta) = 1 - \left[p_0 \times Q\left(\tfrac{-\Theta - A_0}{\sigma}\right) + p_1 \times \left(1 - Q\left(\tfrac{\Theta - A_1}{\sigma}\right)\right)\right] \tag{35.1}$$

The average probabilities of error in the (2, 2), the simple (2, 3) and our modified (2, 3) DMCs are modeled as Q functions as can be calculated as in (20), (33) and (35). We have also discussed the intervals by which the SR effect is observed. The modified (2, 3) exhibits SR for a detection threshold Θ less than the signal amplitude, while the other two DMCs for Θ greater than the signal amplitude [5]. We generated a three dimensional plot to investigate and compare the performances of the three DMCs as shown in Figure 36.

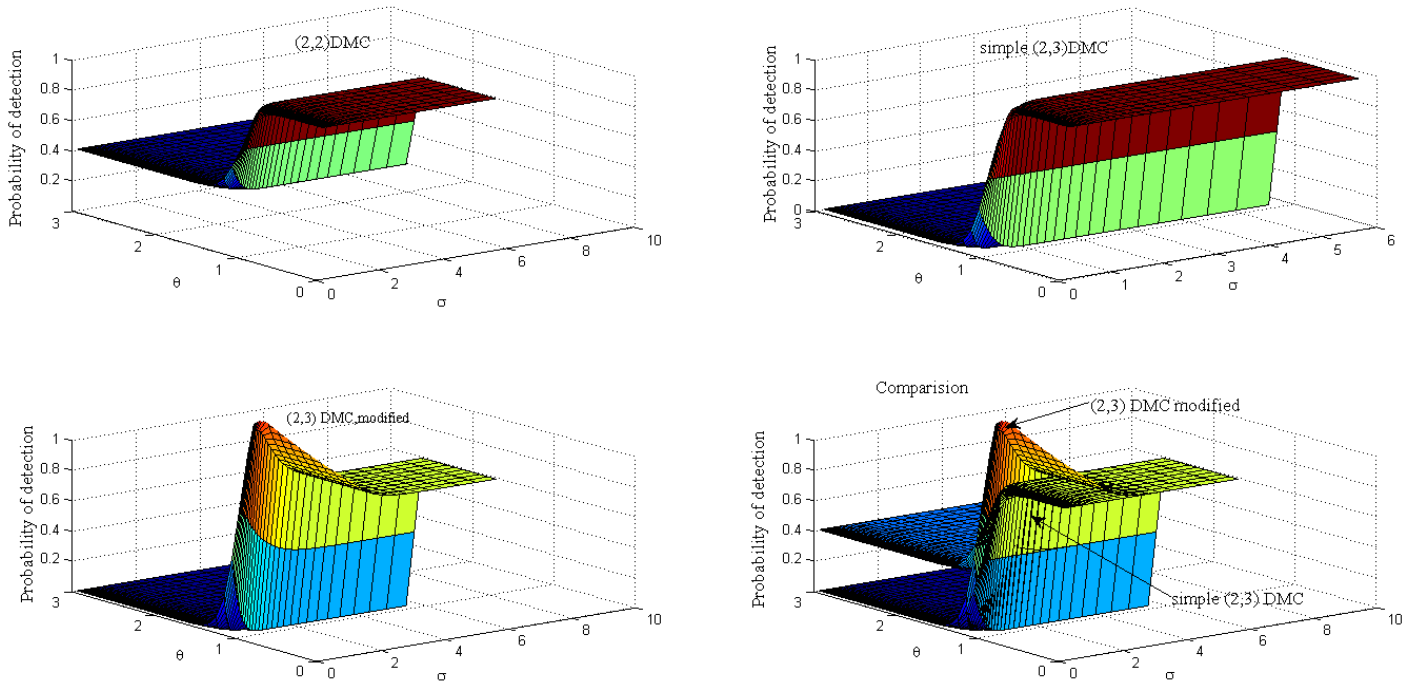

Figure 36: DMCs performance Comparison. Using (20.1), (35.1) and (33.1).

An ideal sensor network is designed to detect a target with negligible probability of false alarm and miss. However, we cannot reach that peak due to channel imperfections. Thus the designer task would be to compare different channel models and come up with a model that minimizes the probability of error relatives to the other feasible channel models. In both (2, 3) DMCs the probability of detection deteriorates so fast as the symmetric decision threshold theta increases far away from the signal amplitude. However, the (2, 2) DMC exhibits slow decay in the probability of detection as the single decision threshold theta increases far away from the signal amplitude. This slow decrease in the probability of detection is from the fact that, increasing the threshold increases the probability of missing a target. But, the reduction in probability of false alarm helps to compensate the increase in the probability of miss, which ultimately balances the average probability of error.

To the best of our knowledge, although many channel models are proposed [3]-[12], we showed our modified (2, 3) DMC has better performance in detecting a target by minimizing the probability of error which is inherent to any communication system. The results of this thesis clearly indicate how one could compare the performance of the (2, 2) and (2, 3) DMCs. We also investigated how one could improve the probability of correct detection in the threshold based communication systems, where local, finite, and relatively finite energy sources are deployed to monitor a geographical area.

4.4.1 Stochastic Resonance and Forbidden Interval Theorem in the case of the BSC

In [14], the Forbidden Interval Theorems (FIT) in stochastic resonance is introduced. The FIT gives the necessary and the sufficient condition for stochastic resonance to occur. In general, the forbidden interval is the region or interval in which there is no stochastic resonance. A similar approach is reported in [15], where the Algebraic Information Theory (AIT) was used for the (2, 2) DMC to determine the forbidden interval. Moreover, in [5] the forbidden interval theorem is expanded into (2, 3) DMC while enhancing the channel capacity by addition of noise.

As our performance measure is the probability of error we studied the noise enhanced signal detection and identify the intervals by which the effect of stochastic resonance is observed. We first analyzeed the (2, 2) DMC to lay down a foundation for the later anaysis of the (2, 3) DMC.

Differentiating (20) with respect to the noise standard deviation σ, we get

$$\frac{\partial p(e|\theta)}{\partial \sigma} = p_0 \frac{\partial \int_{\frac{\theta-A_0}{\sigma}}^{\infty} \frac{1}{\sqrt{2\pi}} * e^{-\left(\frac{x^2}{2}\right)}}{\partial \sigma} - p_1 \frac{\partial \int_{\frac{\theta-A_1}{\sigma}}^{\infty} \frac{1}{\sqrt{2\pi}} * e^{-\left(\frac{x^2}{2}\right)}}{\partial \sigma} \tag{36.1}$$

Simplifying (36.1) we obtain

$$0 = p_0 \times \left(0 - e^{-0.5\left(\frac{\theta-A_0}{\sigma}\right)^2}\right) \times -\left(\frac{\theta-A_0}{\sigma^2}\right) + p_1 \times \left(0 - e^{-0.5\left(\frac{\theta-A_1}{\sigma}\right)^2}\right) \times \left(\frac{\theta-A_1}{\sigma^2}\right) \tag{36.2}$$

$$p_0 \times \left(0 - e^{-0.5\left(\frac{\theta-A_0}{\sigma}\right)^2}\right) \times \left(\frac{\theta-A_0}{\sigma^2}\right) = p_1 \times \left(0 - e^{-0.5\left(\frac{\theta-A_1}{\sigma}\right)^2}\right) \times -\left(\frac{\theta-A_1}{\sigma^2}\right) \tag{36.3}$$

Rearranging we get

$$\frac{p_0 * \left(\frac{\theta-A_0}{\sigma^2}\right)}{p_1 * \left(\frac{\theta-A_1}{\delta^2}\right)} = \frac{e^{-0.5\left(\frac{\theta-A_1}{\sigma}\right)^2}}{e^{-0.5\left(\frac{\theta-A_0}{\sigma}\right)^2}} \tag{36.4}$$

Using logarithm in both sides,we obtain

$$\sigma = \sqrt{\frac{2\theta(A_1-A_0)+{A_0}^2-{A_1}^2}{2\ln\left(\frac{p_0(\theta-A_0)}{p_1(\theta-A_1)}\right)}} \tag{36.5}$$

Thus the optimum noise is as a function of signal amplitude and decision threshold Θ and the prior probabilities.

However, in order (36.5) to be defined then the threshold Θ should be greater than the signal amplitude A_1 and A_0. Thus SR occurs in the interval $A_0<A_1<\Theta$

For the (2, 3) DMC shown in the Figure 36, in order to study the forbidden interval theorem we followed the same procedure as we did with the (2, 2) DMC.

Differentiating (35) with respect to the noise standard deviation σ and rearranging, we get

$$p_0 \times \left(e^{-0.5\left(\frac{\theta-A_0}{\sigma}\right)^2}\right) \times \left(\frac{-\theta-A_0}{\sigma^2}\right) = p_1 \times \left(e^{-0.5\left(\frac{\theta-A_1}{\sigma}\right)^2}\right) \times \left(\frac{\theta-A_1}{\sigma^2}\right) \quad (37.1)$$

Solving for the optimum noise, we get

$$\sigma = \sqrt{\frac{2\Theta(A_1+A_0)+{A_0}^2-{A_1}^2}{2\ln\left(\frac{p_0(-\Theta-A_0)}{p_1(\Theta-A_1)}\right)}} \quad (37.2)$$

The optimum value of the noise obtained in (37.2) is defined if and only if

$$-\Theta < A_0 < A_1 < \Theta$$

The above interval for which the SR phenomena observed is consistent with the intervals by which the channel capacity exhibits SR in [5].

4.4.2The optimum noise for minimum probability of error in the (2, 2) DMC

The noise enhancement for signal detection in the case of (2, 2) DMC depends on the location of the detection threshold relative to the signal amplitude. As it is deduced in (36.5) the threshold theta should be greater than the signal amplitude in order the system to exploit the SR effect. In Figure 37 we observed the optimum noise to be zero a long as the threshold Θ is less than the signal amplitude (A=1). SR cannot happen in this interval. However, for the detection threshold Θ greater than the signal amplitude, as shown in the figure below, there is an optimum value of the noise that contributes to better signal detection.

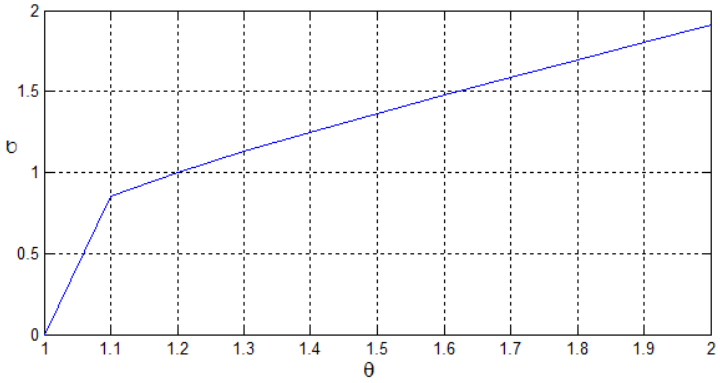

Figure 37: Optimal noise power σ vs threshold Θ. The signal amplitude is 1.

4.4.3 Stochastic Resonance and the modified (2, 3) DMC

Following our work in the case of the (2, 2) DMC and the (2, 3) DMC, we revisited (33)

Rewriting and differentiating (33) with respect to noise standard deviation σ, we get

$$\left(e^{-0.5\left(\frac{A-\theta}{\sigma}\right)^2}\right)\times\left(\frac{A-\theta}{\sigma^2}\right)-\left(e^{-0.5\left(\frac{A}{\sigma}\right)^2}\right)\times\left(\frac{A}{\sigma^2}\right)-\left(e^{-0.5\left(\frac{A-\theta}{\sigma}\right)^2}\right)\times\left(\frac{A-\theta}{\sigma^2}\right)*Q\left(\frac{A}{\sigma}\right)+\frac{A}{\sigma^2}\times$$
$$\left(e^{-0.5\left(\frac{A}{\sigma}\right)^2}\right)\times Q\left(\frac{A}{\sigma}\right)-\frac{A}{\sigma^2}\times\left(e^{-0.5\left(\frac{A}{\sigma}\right)^2}\right)\times Q\left(\frac{A-\theta}{\sigma}\right)+\frac{A}{\sigma^2}\times\left(e^{-0.5\left(\frac{A}{\sigma}\right)^2}\right)\times Q\left(\frac{A}{\sigma}\right)=0 \qquad (38.1)$$

Collecting like terms, we get

$$\left(\frac{A-\theta}{\sigma^2}\right)\times\left(e^{-0.5\left(\frac{A-\theta}{\sigma}\right)^2}\right)\times\left(1-Q\left(\frac{A}{\sigma}\right)\right)=\frac{A}{\sigma^2}\times\left(e^{-0.5\left(\frac{A}{\sigma}\right)^2}\right)\times\left(1-Q\left(\frac{A-\theta}{\sigma}\right)\right) \qquad (38.2)$$

To deduce the interval by which the noise enhancement effect exists we find a relationship in terms of sigma as follows:

$$\sigma=\sqrt{\frac{2\theta A-\theta^2}{2\ln\left(\left(\frac{A}{A-\theta}\right)\times\left(\frac{1-Q\left(\frac{A-\theta}{\sigma}\right)}{1-Q\left(\frac{A}{\sigma}\right)}\right)\right)}} \qquad (38.3)$$

In order (38.3) to be defined then $A>\theta$, i.e. the signal need to superthreshold .

In the special case when the threshold theta,Θ=0, the (2, 3) DMC becomes (2, 2) DMC, and we know this is optimum regardless of the noise..

Chapter 5

Conclusions and future work

In this thesis, we analyzed the (2, 3) DMC and formulated the average probability of error as a function of signal amplitude, threshold theta and noise power sigma. We studied the trade-off between the detection threshold and signal amplitude for the average probability of error. We also studied how the receiver operating characteristics curves in case of the (2, 3) DMC shifts with the detection threshold theta and noise power sigma.

We found the signal has to be subthreshold in the case with BSC and the simple (2, 3) DMC. However, in our proposed (2, 3) DMC model the signal has to be superthreshold. Moreover, we showed our (2, 3) DMC performs better than the simple (2, 3) DMC

In addition, we studied the threshold based stochastic resonance behavior of binary-input ternary-output DMC. The physical communication channel model is used to analyze the average probability of error of the BSC/SE in the context of the stochastic resonance phenomenon in order to investigate SR effect in the modified (2, 3) DMC. We observed the existence of an optimum noise in case of nonlinear systems which is a function of our detection threshold Θ.

To the best of our knowledge, although many channel models are proposed [3]-[12], we showed our modified (2,3) DMC has better performance in detecting a target by minimizing the probability of error which is inherent to any communication systems The results of this thesis clearly indicate how one could compare the performance of the (2,2) and (2,3) DMCs. The result of our work can be used in threshold based communication systems, where local, finite, and relatively finite energy sources are deployed to monitor a geographical area.

As our proposed model deals with a static threshold Θ, the future work can be expanded with dynamic threshold employing the same model. Especially when the precise location of a target is of high importance in the case of distributed wireless sensor networks, it is necessary that we dynamically set the threshold Θ comparing the different reading from the distributed sensors. The rate of true detection to the total detection can be used to dynamically set our threshold Θ. Furthermore it would be more interesting to investigate the effect of noise simultaneously using both information theory and communication channel parameters. Does the optimum value of noise that boosts our signal detection also maximize the channel capacity and mutual information of a channel? Thus, one can optimize the system to efficiently use communication bandwidth and energy which are both scarce in the case of underwater distributed wireless sensor networks.

References

[1] C.E Shannon and W.W Weaver, "The Mathematical Theory of Communication", *University of Illinois Press ,* Urbana, IL, 1949.

[2] F.Ian , Su.Weelian and C.Erdal**,''** A Survey on Sensor Networks**",** *Georgia Institute of Technology*

[3] F. Mu and J. Zhang and J. Du, "A weak signal detection technology based on stochastic resonace''**,** *Computer Science and Service Systems (CSSS)*, International conference, pp. 2004 – 2007, Jun.2011.

[4] P. Cotae," Blind Doppler Estimation and Compensation in the Underwater Communications**",** *Technical report submitted to the Naval Research Laboratories*, Washington DC, Sept. 2009.

[5] R. Kamdem, P. Cotae and I.S. Moskowitz," Threshold based stochastic resonance for the binary-input **ternary** output discrete memoryless channels**",** *Proceedings of the IASTED.Communications,Interent and Information Technology*(CIIT), May2012.

[6] Ira. S. Moskowitz, P. Cotae, P. N. Safier, and D. L. Kang, "Capacity Bounds and Stochastic Resonance **for** Binary Input Binary Output Channels**",** *Proc. of the IEEE Computing, Communications & Applications conference*. pp. 61-66, Jan. 2012.

[7] S. Kay, J. H. Michels, H. Chenand and P.K.Varshney, "Reducing probability of decision error using stochastic**",***IEEE.Trans on Signal processing*. vol.13, pp.695 – 698, Nov.2006.

[8] A. Patel, B.Kosko, "Error probability noise benefits in threshold neural signal detection**",** *Neural Networks, IJCNN*, International Joint conference.pp.2423– 2430, Jun.2009.

[9] S. Bayram, S. Gezici and H. Vincent, "Noise enhanced detection in the restricted Bayesian framework''**,** *IEEE Trans.on Acoustic speech and signal processing,ICASSP*, international conference. March 2010.

[10] A.Patel and B. Kosko, "Optimum noise benefits in neyman-pearson signal detection''**,** *IEEE Trans. on Acoustic speech and signal processing,ICASSP*. International Conference. pp. 3889 – 3892.March.2008.

[11] F. Mu and J. Zhang and J. Du, "A weak signal detection technology based on stochastic resonace''**,** *computer science and service system (CSSS),* International conference, pp. 2004 – 2007, Jun.2011.

[12] A. Patel and B. Kosko, "Stochastic resonance in continuous and spiking Neuron models with levy noise neyman-pearson signal detection''*, IEEE Trans on Neural Networks*.,Volume.19,pp. 1993 – 2008,Dec.2008

[13] H. Chen and P.K.Varshney, "Theory of Stochastic Resonance effect in signal detection-Part II: variable Detector**"**,*IEEE Tran on Signal Processing*..vol. 56, July.2008.

[14] Bart Kosko, Sanya Mitiam, Ashok Patel and Mark M. Wilde, "Applications of Forbidden Interval Theorem in Stochastic Resonance**, "** *In Applications of Nonlinear Dynamics ,Understanding Complex Systems*, pp 71-89.Springer-Verlag, 2009.

[15] Ira S. Moskowitz, Paul Cotae, Pedro N. Safier,"Algebraic Information Theory and Stochastic Resonance for Binary-Input Binary-Output Channels **,"** *Proceedings IEEE 46th Annual Conference on Information Sciences and Systems-CISS 2012,* Princeton University, March 17-19, pp.1-6, March 2012

[16] François Chapeau-Blondeau," Noise Enhanced Capacity via Stochastic Resonance in an Asymmetric Binary Channel**,**" *Physical Review E*, 55(2):2016-2019, 1997.

[17] Paul Cotae and T.C. Yang "A cyclostationary blind Doppler estimation method for underwater acoustic communications using direct-sequence spread spectrum signals**,"** *8th International conf. on Communications*, *COMM 2010*, Bucharest, July 2010

[18] J. Proakis and Masoud Salahi, *' 'Probability of error for M-ary pulse modulation*",*Fundamentals of communication systems*, Pearson Education INC, pp .432-450,2007.

[19] Thomas M. Cover and Joy A. Thomas," Elements of Information Theory," *Second Edition, John Wiley and Sons*, 2006.

[20] Mark Damian McDonnell, "Theoretical Aspects of Stochastic Signal Quantization and Suprathreshold Stochastic Resonance," *PhD thesis, The University of Adelaide*, Australia, Feb.2006